

Chapter 1

An InSAR-based survey of deformation in the central Andes, Part I: Observations of deformation: Volcanoes, salars, eruptions, and shallow earthquake(s)?

Abstract

We extend an earlier interferometric synthetic aperture radar (InSAR) survey covering about 900 remote volcanos of the central Andes (14° - 27° S) between the years 1992 and 2002. Our survey reveals broad (10's of km), roughly axisymmetric deformation at 4 volcanic centers with no previously documented deformation. Two stratovolcanoes are inflating (Uturuncu, Bolivia, and Hualca Hualca, Peru), and another source of inflation is observed between Lastarria and Cordon del Azufre on the border between Chile and Argentina, that is not associated with a volcanic edifice (here called Lazufre). A caldera (Cerro Blanco, also called Robledo) in northwest Argentina is subsiding. We do not observe any deformation associated with eruptions of Lascar, Chile, (including large eruptions in July 2000, December 1993, and April 1993), at 14 other volcanoes that had recent small eruptions or fumarolic activity, or associated with a thermal anomaly (which we observe to be short-lived) at Chiliques volcano. Inflation at Hualca Hualca stopped in 1997, perhaps related to a large eruption of nearby Sabancaya volcano in May, 1997, although there is no obvious relation between the rate of deformation and the eruptions of Sabancaya. In addition to volcanic deformation, we find several other sources of deformation, including a possible shallow earthquake in Chile and heterogeneous swelling and subsidence at several salt flats (salars) within our study area, particularly the Salar de Atacama. Deformation is observed near volcanoes Hualca Hualca and Coropuna in southern Peru, possibly related to subsurface water flow induced by the nearby M_w 8.4 June 23, 2001, Arequipa earthquake. Other shallow sources of deformation are also observed in and around the Andahua Valley of southern Peru, presumably related to hydrological activity.

1.1 Introduction

The central Andes (14°-28°S) has a high density of volcanoes (Figure 1.1), but a sparse human population, such that the activity of most volcanoes is poorly constrained (e.g., *de Silva and Francis*, 1991). For example, *Simkin and Siebert* (1994) list 15 different volcanoes that have erupted in the central Andes during the past century, but at least one report is probably wrong (*Smithsonian Institution*, 1997b), and several other “eruptions” might only be increased fumarolic activity (*Simkin and Siebert*, 1994). Furthermore, subtle signs of activity, such as heightened fumarolic activity, are infrequently reported for only a few edifices (e.g., *Gonzalez-Ferran*, 1995; *Smithsonian Institution*, 1996b, 1993d).

It is desirable to monitor subtle changes at volcanoes, especially surface deformation, in order to determine whether magma is moving at depth. In some cases, particularly at basaltic volcanoes like Kilauea, Hawaii and Krafla, Iceland, eruptions have been preceded by surface inflation due to magma injection at depth (e.g., *Dvorak and Dzurisin*, 1997). This simple relation between deformation and eruption is not the norm, especially at stratovolcanoes (*Dvorak and Dzurisin*, 1997), common in the central Andes. Therefore, a history of deformation and eruption must be established for each volcano. For the hundreds of remote volcanos of the Central Andes, satellite interferometric synthetic aperture radar (InSAR) is currently the most viable way to establish the background level of activity.

InSAR measures the change in path length in the satellite line-of-sight (LOS) between observations. Many factors contribute to changes in path length, but with appropriate removal of topographic effects and if atmospheric and ionospheric effects are small and/or can be isolated, path length changes correspond to deformation of the Earth’s surface (e.g., *Rosen et al.*, 2000). We use ERS-1 and ERS-2 satellite radar images with a spatial resolution of 20 m and image extents greater than 100 km, such that deformation can be monitored at scores of volcanoes in each scene at high spatial resolution. We complement the ERS data with data from the JERS radar satellite.

We use InSAR to extend our systematic observations of deformation at nearly 900

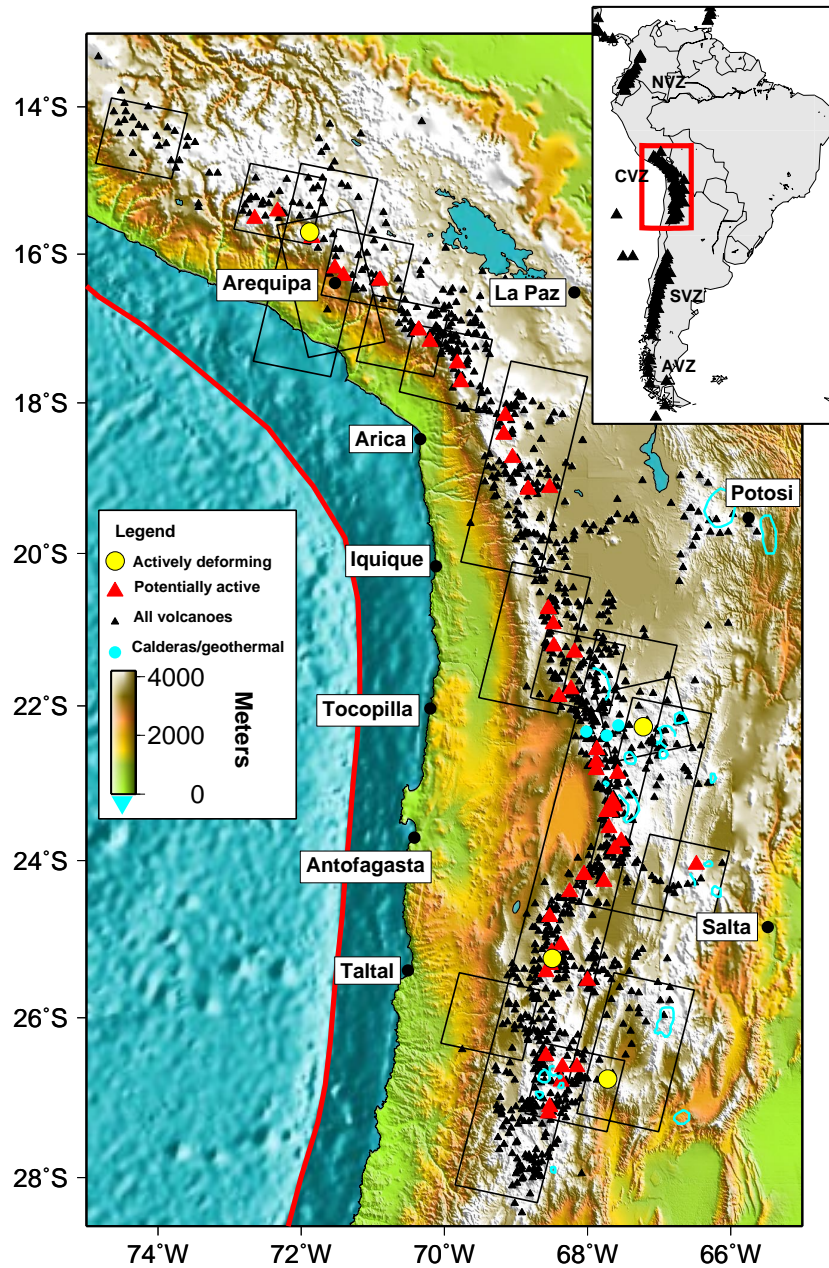


Figure 1.1: Shaded relief map of the Central Andes including the 1,113 potential volcanic edifices compiled by *de Silva and Francis* (1991) (black triangles), and “potentially active” volcanoes of *de Silva and Francis* (1991) plus other volcanoes found to be active since their study (red triangles). Yellow circles show actively deforming volcanoes found in this study. Light blue circles show location of geothermal fields. The light blue lines outline the large silicic calderas listed by *de Silva and Francis* (1991) and *Riller et al.* (2001). Reference map in upper right shows study area (red box) in the Central Volcanic Zone (CVZ) relative to the other South American volcanic belts – Northern Volcanic Zone (NVZ), Southern Volcanic Zone (SVZ) and the Austral Volcanic Zone (AVZ). Major cities are indicated. The red line in the ocean is the location of the subduction zone trench. Black square outlines show the location of radar data used in this study.

volcanoes in the central Andes (*Pritchard and Simons, 2002*) between 1992 and 2002 to determine which volcanoes might have magma moving at depth. In this chapter, we detail the data used in the survey, including additional data and data reprocessed with digital elevation models (DEM) from the Shuttle Radar Topography Mission (SRTM), the accuracy of the measurements, document the non-volcanic deformation discovered, and discuss the implications of the constraints we impose on deformation during several volcanic eruptions. In the next chapter, we discuss the results of modeling the deformation, the physical cause of the deformation, and implications for the rate of magmatic additions to the volcanic arc.

By surveying a large number of volcanoes with InSAR, we can begin to answer questions that were once intractable – within a large area, how many volcanoes are deforming at a given time, are their magma source depths uniform, and how time-dependent is the deformation? Some studies have noted a possible correlation between earthquakes and volcanic eruptions, particularly in South America (e.g., *Gonzalez-Ferran, 1995*), but with InSAR, we can look for earthquake-volcano interaction that does not result in an eruption, such as subtle changes in the rate of deformation. A particular advantage of InSAR over ground surveying (such as GPS) is that we can survey all volcanoes within a scene, instead of only a handful of selected targets. In our preliminary survey, we reported four centers of active deformation, but none of them were on lists of potentially active volcanoes in the central Andes (with one possible exception, see below), and might have been missed without the large spatial coverage of InSAR (*Pritchard and Simons, 2002*).

1.2 Data used

While many of the volcanoes are permanently snow-capped because of their high elevations (dozens exceed 6000 m), the central Andes is generally well suited for the application of InSAR, because the region is generally arid, cloud free, and has little vegetation. The lack of rainfall, vegetation, and human cultivation improves the InSAR measurements, which rely upon the radar scattering properties of the Earth's

surface remaining the same between observations. In other words, the amplitude and phase at a given pixel within the radar image at the time of the first observation must be coherent with the amplitude and phase at the time of the second observation. A high coherence (close to 1) means that the ground surface has changed little on the scale of the radar wavelength between measurements, while a low coherence (near 0) indicates that precipitation, wind, vegetation, or human activities have changed the surface reflective properties at the scale of the radar wavelength.

In Figure 1.2, we map the interferometric coherence in the central Andes. Interferometric coherence is wavelength dependent, such that longer wavelengths (e.g., the L-band at 24 cm wavelength) retain their coherence over longer time periods than the C-band data used here (e.g., *Rosen et al.*, 1996). We observe good interferometric correlation near the arid coast, but poorer correlation in mountainous areas. There also appears to be a north-south trend with better correlation south of 21°S, where the zone of good correlation along the coast is wider than in southern Peru. The coast-inland and north-south variations in correlation are presumably related to regional climate variations, with more precipitation falling in the north (related to the “Bolivian winter” meteorological effect) and in mountainous areas (e.g., *de Silva and Francis*, 1991; *Montgomery et al.*, 2001). Generally, coherence is lost on the stratovolcano edifice because precipitation is more likely to fall there than on the surrounding lower lying areas, and the steep slopes promote small scale movement. However, InSAR measurements of deformation are possible in almost all regions of low correlation within our study area where we apply spatial averaging (*i.e.*, “looking down” the interferogram) at the expense of spatial resolution.

We selected ERS-1/ERS-2 radar data to maximize coverage of the 44 “potentially active” volcanoes determined to have been the most active since the last glacial maximum (about 10,000 years ago) on the basis of satellite mapping (*de Silva and Francis*, 1991). In addition to their 44 “potentially active” volcanoes, we added volcanoes that might have erupted during the last century (*Smithsonian Institution*, 1993a; *Simkin and Siebert*, 1994) for a total of 53 volcanoes on our list (see the electronic Appendix). *Gonzalez-Ferran* (1995) lists 84 “active volcanoes,” although his criteria are not as

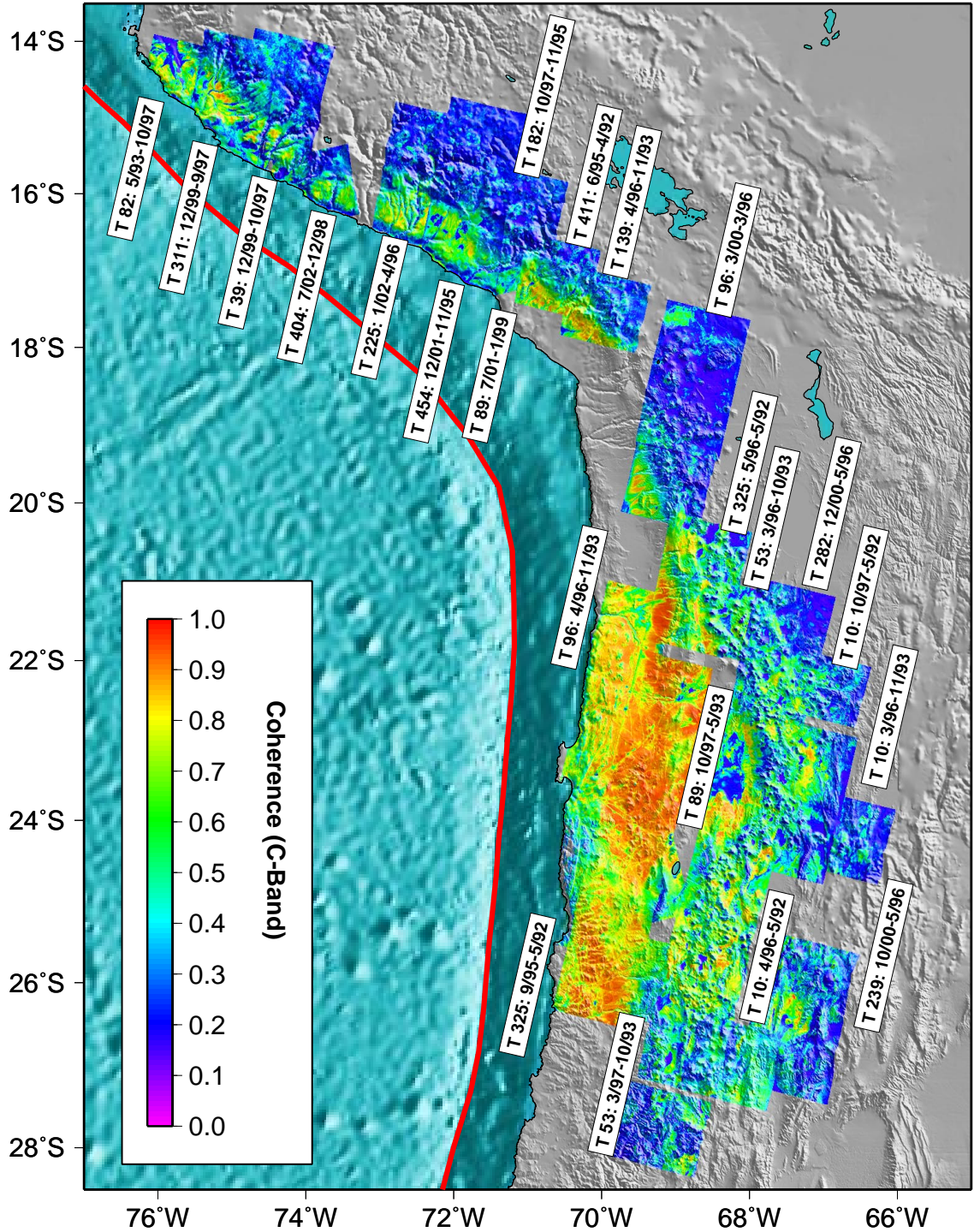


Figure 1.2: Interferometric coherence for ERS C band radar (wavelength = 5.6 cm) for the area where we have studied tectonic and volcanic deformation in west-central South America. The data in this figure is from this study and our other studies of earthquake deformation (Chapters 3, 4 and 5).

clearly defined as *de Silva and Francis* (1991). There is much overlap, and we ended up surveying 78 of the 84 volcanoes of *Gonzalez-Ferran* (1995), and all 53 from the augmented list of *de Silva and Francis* (1991) (see Table 1.1).

de Silva and Francis (1991) grouped the 1,113 volcanic edifices in the central Andes into different age groups based on their geomorphological characteristics. As the authors note, it is difficult to convert the geomorphological ages into actual ages because the state of preservation of each edifice depends on its composition and local climate. For example, the local climate variations have caused extensive glaciation in the north of the arc while no obvious evidence of glaciation exists south of 24°S (*de Silva and Francis*, 1991). However, using geochronological data from a few edifices, several authors have inferred that one of the *de Silva and Francis* (1991) morphological classes corresponds to volcanoes less than 250,000 years old, another class to those less than 1-2 Ma, and that the entire database includes volcanoes less than 10-20 Ma (*Baker and Francis*, 1978; *de Silva and Francis*, 1991; *Francis and Hawesworth*, 1994).

Morphological age ¹	Estimated age (yrs)	# edifices ¹	# surveyed (%)	Mean yrs/volc	Cumulative volcano-years
1-5	< 10-20 Ma ^{2,3}	1,113	932 (84%)	6.3	5,888
1-2	< 1-2 Ma ²⁻⁴	390	353 (91%)	6.6	2,326
1	< 10,000 ⁵	112	108 (96%)	6.8	729
“potentially active”	< 10,000 ⁵	53 ⁶	53 (100%)	7.1	376

Table 1.1: The number of volcanoes surveyed for deformation and the timespan of data coverage for different geomorphological classes of volcanoes. Relating geomorphological features to age is notoriously difficult (see text) and is at best accurate within a factor of two. For some volcanoes, the effective timespan is increased by overlapping data from the same orbital track that can be stacked together, but this effect is not accounted for here. In addition, some volcanoes are imaged in multiple orbital tracks. Data sources for table: ¹*de Silva and Francis* (1991), ²*Francis and Hawesworth* (1994), ³*Wörner et al.* (2000), ⁴*Baker and Francis* (1978), ⁵These volcanoes lack glacial features, so have presumably been active in the last 10,000 years, although the volcanoes are probably older than this and likely at least 250,000 years old (*Francis and Hawesworth*, 1994). ⁶The original list of potentially active volcanoes (*de Silva and Francis*, 1991) has been augmented by this study (see text).

Table 1.1 shows a summary of the total number of volcanoes we surveyed of each age and the temporal coverage. We surveyed 931 edifices for a total of about 5900 volcano-years, or 353 volcanoes less than 1-2 Ma for about 2300 volcano-years. There are many large silicic calderas in the central Andes, especially in the Altiplano-Puna Magmatic Complex (APMC) located between 21-24°S (*de Silva*, 1989) where the largest known magma body in the continental crust has been seismically imaged (*Chmielowski et al.*, 1999; *Yuan et al.*, 2000; *Zandt et al.*, 2003). We surveyed deformation at 17 known calderas (*de Silva and Francis*, 1991; *Riller et al.*, 2001) and three geothermal fields. We sought data for each edifice during the entire period when radar data was available (1992-2002), but this was not possible due to constraints on data availability (Figure 1.3). In total, we used about 160 scenes of radar data to create more than 80 interferograms, most of which can be viewed as part of the electronic Appendix.

We process the radar data using the Caltech/JPL InSAR package, ROI_PAC. We use satellite orbital information, accurate to about 20 cm, from the Delft Institute for Earth-Oriented Space Research (*Scharroo et al.*, 1998). We remove topographic effects with both the 2-pass approach where a pre-existing DEM is used, and the 4-pass approach using ERS-1/2 tandem data – *i.e.*, separated in time by one day. We process every interferogram using the 2-pass approach, but also use the 4-pass approach when tandem data is available, to check for atmospheric effects and phase unwrapping errors in the tandem data.

We encountered several minor problems in processing the data: 1) We had difficulty fixing missing lines from orbit 25320 of ERS-1, because the line counter in the raw data was wrong. However, use of the satellite clock and hand editing of the raw data allowed us to correct most of this problem (e.g., *Pritchard et al.*, 2002). 2) The Doppler centroid changes sign from time to time within our study area (*i.e.*, <http://earthnet.esrin.esa.it/eo4.135>), so we empirically corrected for this time variable doppler centroid in order to process most scenes. 3) Because precise ERS-1 orbits are not available for 1997, we had to use more crude estimates of orbital locations for initial processing, and then re-estimated the baseline directly from the data using a

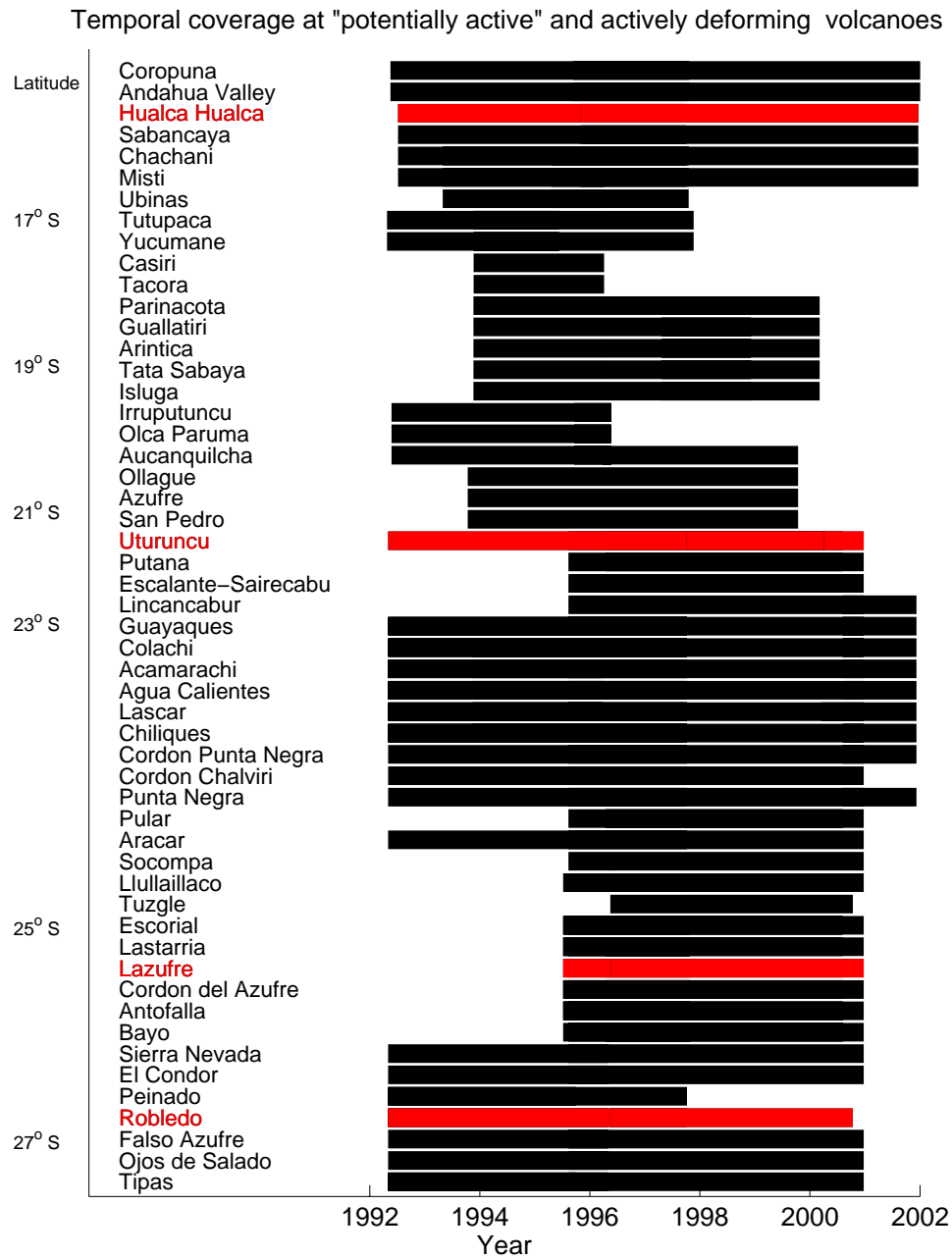


Figure 1.3: Temporal coverage of InSAR data for our volcano survey (53 “potentially active” volcanoes, see text) arranged from north to south (latitudes are along the y axis). Actively deforming volcanoes found with this survey are indicated in red.

synthetic interferogram made with a DEM (*Rosen et al.*, 1996).

1.3 Field work

We have participated in field surveys of some of the central Andean volcanoes to better understand the relation between remote sensing and ground indicators of activity. From October 25-29, 2002, Jose Naranjo, Jorge Clavero and Jorge Cañuta of the Chilean Servicio Nacional de Geología y Minería (Sernageomin), and Mark Simons and Matt Pritchard of Caltech visited several volcanoes in northern Chile. We spent October 25-28 near Lastarria volcano, surveying the activity at Lastarria, and looking for activity from Lazufre and Cordon del Azufre. The group also spent October 29, near Chiliques volcano looking for signs of activity, and talking with local residents about recent observations of the volcano. A seismometer was installed for several hours at Lastarria and Chiliques. Samples were collected at Lastarria and Chiliques in order to date lava flows and pyroclastic deposits.

From April 1-6, 2003, an international group visited Uturuncu volcano, Bolivia. The group measured the temperature of the fumaroles, installed a vertical-component seismometer in several locations, and collected several lava samples. The group included Mayel Sunagua and Ruben Muranca of the Bolivian Servicio de Geología y Minería, Jorge Clavero of Sernageomin, Steve McNutt of the Alaska Volcano Observatory, Fairbanks, Alaska, Catherine Annen, Madeleine Humphreys, Anne le Friant, R. S. J. Sparks of the University of Bristol, and Matt Pritchard of Caltech.

1.4 Results

As reported in our preliminary study, of the 900 hundred volcanoes surveyed, we found broad (10's of km), roughly axisymmetric, centimeter-scale deformation at four centers with no previously documented deformation (*Pritchard and Simons*, 2002). In this section we will more thoroughly document the quality of the data and the criteria used to differentiate deformation from noise. To convey the quality of the interfer-

ograms, and the relation of atmospheric artifacts to topography, we have placed 70 interferograms draped over shaded relief in an electronic Appendix. Figure 1.4 shows the volcanic deformation within the regional setting, as well as higher resolution interferograms at each center draped over local relief. Two stratovolcanoes are inflating (Uturuncu, Bolivia, and Hualca Hualca, Peru), and another source of inflation is seen between Lastarria and Cordon del Azufre on the border between Chile and Argentina, that is not associated with a volcanic edifice (which will hereafter be called “Lazufre”). A caldera (Cerro Blanco, also called Robledo) in northwest Argentina is subsiding.

None of the deforming sources were listed as active volcanoes, although Hualca Hualca, Peru, and Lazufre could be related to other, well known volcanoes (see below). While the four actively deforming volcanoes have had no known eruptions, Lascar, Chile, has erupted several times, but we do not observe deformation between 5/1992-12/2001. We found no measurable deformation at other volcanoes that had documented small eruptions or fumarolic activity during the period when radar observations were made – Ubinas (Peru) (*Smithsonian Institution*, 1996a), Guallatiri (*Smithsonian Institution*, 1996b), Irruputuncu (*Smithsonian Institution*, 1997b), Aracar (*Smithsonian Institution*, 1993a), and Ojos del Salado (*Smithsonian Institution*, 1993d) (all in Chile). The eruptions at Sabancaya, Peru, (*Smithsonian Institution*, 1994a, 1995, 1997a, 1998a,b,c, 2000a) will be discussed in detail below. Further, we did not observe deformation at other volcanoes with known fumarolic activity, although no activity was documented during the period of radar observations (Misti, Tutupaca, both in Peru; Tacora, Isluga, Olca and Paruma, Aucanquilcha, Ollague, San Pedro, Putana, Lastarria, all in Chile, *de Silva and Francis*, 1991, J. Clavero and J. Naranjo, personal communication, 2002).

We observe several non-volcanic sources of deformation, including heterogeneous swelling and subsidence at several salt flats (salars), a possible shallow earthquake in Chile, possible hydrological activity in volcanic areas associated with a large subduction zone earthquake, and some sources of unknown origin in southern Peru. A more detailed discussion of each individual volcanic and non-volcanic source of deformation, and the eruptions of Lascar and Sabancaya follows in later sections.

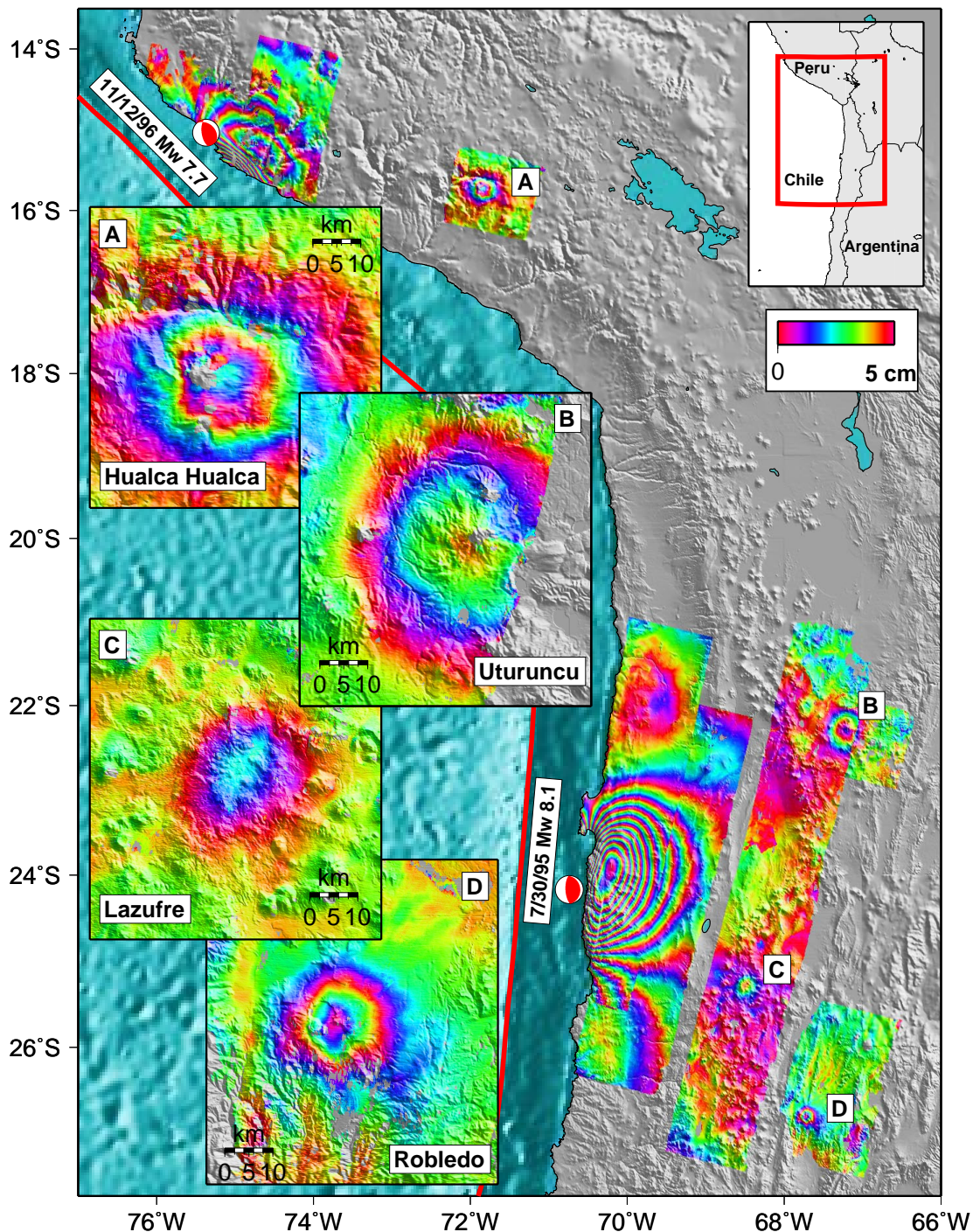


Figure 1.4: Color contours of ground deformation draped over shaded relief from 2 subduction zone earthquakes along the coast and four volcanic centers. Each contour corresponds to 5 cm of deformation in the radar line-of-sight direction. Inset maps show higher resolution interferograms at the four centers of active deformation, showing the relation of the center of deformation to the location of local edifices: a. Hualca Hualca, Peru, time span June 1992-April 1996 (3.9 yr), inflating; b. Uturuncu, Bolivia, time span May 1996-December 2000 (4.6 yr.), inflating; c. Lazufre, border of Chile and Argentina, time span May 1996-December 2000 (4.6 yr), inflating; d. Cerro Blanco (Robledo), Argentina, time span May 1996-October 2000 (4.4 yr), deflating. Reference map in upper right corner places study area in regional context.

We find that a small fraction of all volcanoes in the central Andes are presently deforming. However, it is possible that other volcanoes are deforming at rates that are below our detection threshold. Even where coherence is high and the phase can be unwrapped, sensitivity is not the same in all locations because of variations in atmospheric noise, and the amount of redundant data available that can be used for averaging. By adding many interferograms together (*i.e.*, stacking), we can increase the signal-to-noise ratio, assuming that the noise is uncorrelated between interferograms (e.g., *Zebker et al.*, 1997; *Sandwell and Price*, 1998; *Fialko and Simons*, 2001; *Peltzer et al.*, 2001). Because of the paucity of radar acquisitions in the central Andes, it is difficult to stack many interferograms together, although we have done this where possible.

The accuracy of InSAR measurements has been poorly constrained (but see *Hanssen*, 2001; *Jónsson*, 2002; *Emardson et al.*, 2003). Direct comparison of InSAR with GPS observations (which have their own errors) for several large earthquakes indicates cm-scale accuracy (e.g., *Massonnet et al.*, 1993; *Zebker et al.*, 1994; *Fialko et al.*, 2001b, Chapter 3), and in ideal circumstances, sub-cm accuracy is possible (*Zebker et al.*, 1997). Within our study area, we estimate accuracies of about 1-2 cm over length scales at least 10 km in size, although differentiating such a signal from atmospheric noise can be difficult.

We base our estimate of accuracy on: (1) the ability to detect a “known” signal at Hualca Hualca and Uturuncu within a short period interferogram. We claim that the signal is “known” because deformation was observed in longer period interferograms spanning the same time interval, and we assume the rate of deformation is nearly constant over the given time period – a reasonable assumption, see below; (2) Comparison of interferograms containing deformation that cover essentially the same time period, including interferograms at Cerro Blanco that differ by only 1 day (made using a tandem pair); and (3) The size of the residual from our model fits is usually less than a centimeter. There is a correlation between accuracy and latitude, both because atmospheric effects are larger and coherence is lower north of about 21°S (most likely related to climatic variations, as previously discussed).

Our longest interferograms span about five years (limited by data availability and maintaining interferometric coherence). Thus, with a sensitivity of 1-2 cm per interferogram, we estimate a detection threshold of about 4 mm/yr, assuming the deformation rate is constant. With stacking, we have achieved effectively ten year interferograms in a few locations (e.g., tracks 454, 325, and 96), but since the atmospheric noise is higher in these locations in the northern part of our study area, we still estimate that a signal above 4 mm/yr is required. We think that deformation with smaller rates can be detected if the signal is spatially discontinuous, for example, at the edge of a salt flat (see below), although care is required to ensure that such a signal is not an unwrapping error.

There are two components to atmospheric noise – turbulent mixing and vertical stratification (*Hanssen, 2001; Ewardson et al., 2003*). Vertical stratification is especially important, particularly variations in water vapor, because the phase delays associated with that atmospheric signal can make regions of elevated topography (like volcanoes in the Andes) appear to be moving up or down (e.g., *Zebker et al., 1997; Fujiwara et al., 1998*). In principle, radiosonde and/or GPS observations may be used to correct the InSAR data for the tropospheric effects (*Delacourt et al., 1998; Hanssen, 2001*), but such data does not exist over the central Andes, and the density of such observations is usually much coarser than the 20 m pixel size of InSAR. Instead, we use four criteria to judge whether a signal is atmospheric or surface deformation. For this discussion, we define a “signal” to be a region many pixels in size that has a phase that is more than half a fringe different than surrounding areas. We think that failing all criteria makes a persuasive, although not conclusive, case for atmospheric contamination. It is possible that further data will reveal that several signals that we ascribed to atmosphere were actual surface deformation.

The criteria we use for differentiating between atmospheric effects and surface deformation are as follows: (1) Is the signal observed in independent interferograms, and does it have the same sign? Atmospheric effects can be isolated using pair-wise logic – *i.e.*, forming several interferograms with each individual scene to determine which one contains the anomalous signal (*Massonnet and Feigl, 1998*). Pair-wise logic can

only be used where several interferograms spanning the same time interval exist, and this is not possible for most of the central Andes because of the lack of available data. If two independent interferograms over an identical time period show signals with different signs, it is clearly atmospheric. Because volcanoes have been observed to move up and down (e.g., *Lowry et al.*, 2001a), it is harder to rule out sign changes in temporally non-overlapping or only partially overlapping interferograms. (2) Do nearby edifices show the same pattern? An atmospheric origin is the simplest explanation for many adjacent edifices with similar topography, the same magnitude signal, and/or having a signal that changes sign in unison. (3) Is the deformation pattern confined strictly to the edifice itself, or does it extend far beyond it? If the signal is strongly correlated with topography, this suggests an atmospheric origin. A source beneath a volcanic edifice might cause deformation that is correlated with topography, but unless the source is very shallow (*i.e.*, 1-2 km below the surface, or within the edifice itself), the deformation pattern will be much broader than the volcano. Thus, our method is most sensitive to large-scale deformation from deep sources (> 1 km deep, depending on the size of the edifice). A signal not correlated with topography could be deformation, or it could be atmospheric turbulence, so independent interferograms are necessary – criteria (1). (4) What is the magnitude of the signal? *Hanssen* (2001) predicts that the maximum signal due to atmospheric stratification is of order 4 cm (about 1.5 fringes for ERS). Under extreme conditions, the atmospheric signal could be larger (*Beauducel et al.*, 2000; *Puglisi and Coltelli*, 2001), but we would expect to see the same effect at all nearby edifices with similar topography – criteria (2). The deformation signal at all our actively deforming volcanoes is more than 5 cm. While the spatial character of the deformation field appears to be affected by atmosphere at all four centers of active deformation (especially at Hualca Hualca, see below), we do not think that the entire signal is atmospheric, because all four criteria are satisfied at all four actively deforming volcanoes.

1.4.1 Deforming volcanoes

1.4.1.1 Uturuncu

This stratovolcano lying in southwestern Bolivia, was observed to have weak active fumaroles (*Fernández et al.*, 1973) near the summit (temperatures $< 80^{\circ}\text{C}$ in April 2003). *Kussmaul et al.* (1977) claimed that Uturuncu has lava flows overlying glacial moraines, but such features were not seen in satellite images (*de Silva and Francis*, 1991), or during a field survey in April, 2003 (J. Clavero and S. Sparks, personal communication, 2003). Like many of the volcanoes in the area, there has been some sulfur mining on the edifice. We have made a total of 12 interferograms for Uturuncu covering May 2, 1992 to December 24, 2000 – 11 interferograms from two tracks of descending data and one interferogram from one track of ascending data. Uturuncu is deforming during the entire time interval at a maximum rate between 1-2 cm/yr in the LOS direction (assuming that the deformation rate is constant during the time period of the interferogram).

We detected shallow seismic activity at Uturuncu during a field visit in April, 2003. We occupied six different locations with a single vertical component seismometer courtesy of Steve McNutt, Alaska Volcano Observatory, for a total of more than 24 hours. During the first two hours we recorded nearly 30 earthquakes. The rate of seismicity was less during other time intervals, but was still several events per hour. Many of the earthquakes looked identical, with an S-P time of about 1.2 seconds. We interpret this to mean that they come from a shallow source of persistent seismicity. By moving the seismometer to different locations, we obtained a crude location of this source of persistent seismicity to be about 7 km northwest of the Uturuncu summit (near the center of the deformation source). However, the earthquakes we detected are much shallower than the inferred source of deformation (Figure 2.7). The earthquakes could be related to shallow hydrologic or hydrothermal activity, but further monitoring is necessary to test this hypothesis. Although we observed fumaroles and hot springs, there were no other signs of activity at this volcano, and no indications of eruption in the last 10,000 years.

The high rate of seismicity at Uturuncu is surprising considering the low rate of seismicity at other dormant volcanoes. InSAR has been used to detect non-eruptive deformation at South Sister, Oregon (*Wicks et al.*, 2002), Westdahl, Aleutians (*Lu et al.*, 2000c), and Mount Peulik, Alaska (*Lu et al.*, 2002c). The last eruption of Westdahl was in 1991, of Peulik was in 1814, and no historic eruptions are known for South Sister. There are seismic arrays at Westdahl and South Sister, and Mount Peulik is 50-70 km from a seismic array associated with Mount Katmai. The rate of seismicity at these volcanoes seems to be a few events a year or less (e.g., *Dixon et al.*, 2002, <http://www.geophys.washington.edu/SEIS/PNSN/SISTERS/>, S. McNutt, personal communication, 2003).

1.4.1.2 Hualca Hualca

This edifice is a member of a group of three stratovolcanoes, (Ampato and Sabancaya are the others) in southern Peru. Sabancaya is the youngest and is the most active. Recent activity at Sabancaya began with increased fumarolic and seismic activity in 1985-1986, a major period of eruptions between May 1990 and early 1992 (e.g., *Smithsonian Institution*, 1988, 1990a,b,c, 1991a,b; *de Silva and Francis*, 1991; *Chorowicz et al.*, 1992; *Simkin and Siebert*, 1994; *Gonzalez-Ferran*, 1995), and several small eruptions and persistent fumarolic activity throughout the 1990's (*Smithsonian Institution*, 1994a, 1995, 1997a, 1998a,b,c, 2000a) that has led to melting of its ice cap. Ash from the eruptions has increased melting at Hualca Hualca (leading to mudflows, *Smithsonian Institution*, 1990a, 1991a) and Ampato (where an Incan ice mummy was found). Activity at Hualca Hualca has been more limited than at Sabancaya – it is known to have active fumaroles (*Gonzalez-Ferran*, 1995), and activity at a parasitic cone on Hualca Hualca was suspected prior to our observations (M. Bulmer, personal communication, 2001). The relationship between deformation near Hualca Hualca and the eruptions of Sabancaya are discussed in more detail below.

Of the four actively deforming volcanoes, a few interferograms at Hualca Hualca show the most distortion by atmospheric effects, and we have taken this into consideration when modeling, see Chapter 2. We have made 16 interferograms from one track

of descending ERS radar data, 1 interferogram from an ascending track of ERS data, and 3 interferograms using JERS data. Because the JERS satellite uses a longer radar wavelength (L band: 24 cm) than ERS, it is less sensitive to deformation. Given the short time period of observation available (interferograms spanning 1996-1994, shown in the Appendix) compared to the deformation rate, a signal would be barely above the detection threshold. We have stacked the two longest JERS interferograms to improve the signal-to-noise ratio. Together, the data span June 2, 1992 to December 21, 2001, and while the deformation rate was about 2 cm/yr between 1992 and 1997, there is no apparent deformation from a deep source after 1997 (Figure 1.5, see the discussion about Sabancaya below).

1.4.1.3 Lazufre

A surprising result of our volcano survey was the discovery of a source of deformation not associated with any known edifice, but lying between between the “potentially active” centers of Lastarria and Cordon del Azufre (*de Silva and Francis, 1991*), along the border between Chile and Argentina. No activity has been recorded at Cordon del Azufre, but fumarolic activity has been observed at Lastarria (*de Silva and Francis, 1991*). The northernmost crater is the most active (*Gonzalez-Ferran, 1995*) – in fact, activity at Lastarria is thought to be generally migrating to the north (*Naranjo and Francis, 1987*), while the observed deformation is to the south. Lastarria has been more studied than Cordon de Azufre, because of its unusual sulphur lava flows (*Naranjo, 1985*), and large debris avalanche (*Naranjo and Francis, 1987*). No active fumaroles were observed at Cordon del Azufre, or between Lastarria and Cordon del Azufre in the vicinity of the Lazufre magma body during a field visit in October, 2002. The activity at Lastarria in October, 2002 seems similar to that observed in the late 1980’s (J. Naranjo, personal communication, 2002). The maximum temperature at the fumaroles was the same in October 2002 and in the late 1980’s, about 293°C (J. Clavero, personal communication, 2002). We have made 7 interferograms from a single track of descending ERS data spanning August 12, 1995 to December 24, 2000. We do not observe deformation in two interferograms spanning times before 1998, but

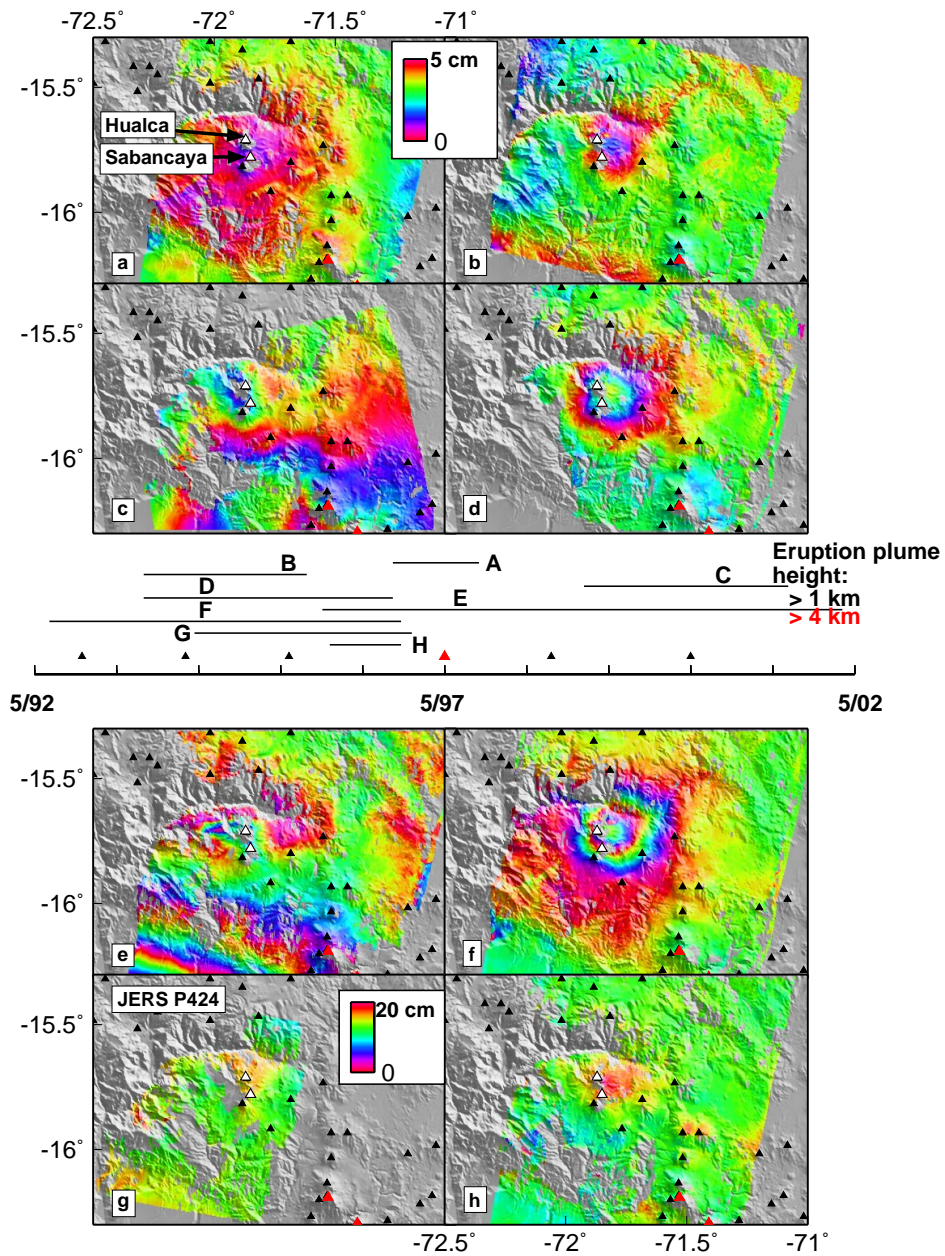


Figure 1.5: Interferograms spanning eruptive activity at Sabancaya showing deformation at Hualca Hualca (both volcanoes shown as white triangles) from one track of ERS data and one path from JERS. In the center of the figure, the time period of the interferograms and eruptions of Sabancaya are shown (*Smithsonian Institution, 1994a, 1995, 1997a, 1998a,b,c, 2000a*). The height of the eruption cloud above the edifice summit can be used to define the explosivity of the eruption (VEI, *Simkin and Siebert, 1994*). Note that the “eruptions” in August-September, 1998 and April-May, 2000 are represented as discreet events, but are in reality continuing activity. The fringes not related to Hualca Hualca and Sabancaya in c and e are from the June 23, 2001, M_w 8.4 Arequipa earthquake. In these two interferograms, there is no clear signal from the deep magma chamber, although there is clearly a region of localized subsidence to the northwest of Hualca Hualca in e (see text). Other symbols are the same as in Figure 1.1.

we see deformation at a rate of at least 1 cm/yr (because the deformation was not uniform in time) in the LOS is seen in three interferograms spanning 1995/1996-2000.

1.4.1.4 Cerro Blanco (Robledo)

This caldera, located in northwest Argentina, is unusual among the actively deforming volcanoes because it is subsiding. The caldera is called Cerro Blanco on Argentinian maps (J. Viramonte, personal communication, 2002), but called Robledo in the Smithsonian Institute's database (*Simkin and Siebert, 1994*). *de Silva and Francis (1991)* call the caldera Robledo and the silicic dome in the southwest corner of the caldera Cerro Blanco. Henceforth, we call the caldera Cerro Blanco. We have made 7 interferograms from 2 descending tracks spanning May 2, 1992 to October 12, 2000, and during that time, the maximum rate of deformation in the LOS decreased from about 2.5 to 2 cm/yr.

1.4.2 Selected non-detection

1.4.2.1 Chiliques

Nighttime thermal infrared images taken by the ASTER (Advanced Spaceborne Thermal Emission and Reflection Radiometer) instrument on the Terra satellite indicated a thermal anomaly at Chiliques volcano (a Chilean stratovolcano within our study region) on January 6, 2002, but not on May 24, 2000 (http://www.jpl.nasa.gov/releases/2002/release_2002_85.html). Our further analysis of the ASTER nighttime thermal infrared images indicates that the thermal anomaly was probably short-lived. An anomaly was seen on April 5, 2002, but no anomalies were seen between May-September, 2000 (data from 7/27, 8/12, and 9/13) or May-July, 2002 (data from 5/23, 6/15, 6/24, 7/17). No features were seen in any of the six short-wavelength infrared bands, indicating a low-temperature thermal anomaly, and a more detailed study is underway (M. Abrams, personal communication, 2002). No fumarolic activity was seen during a field visit to the base of Chiliques in October, 2002, or was noted by the villagers of Socaire, 15 km from Chiliques and the closest settlement to the vol-

cano (J. Naranjo and J. Clavero, personal communication, 2002). No deformation is observed at Chiliques between 5/1992-12/2001 (Figure 1.6).

1.4.3 Eruptions

1.4.3.1 Lascar

Lascar, Chile, is currently the most active volcano in the central Andes, and although it has had several major and minor eruptions during the period when InSAR data is available, no pre-eruptive, co-eruptive, or post-eruptive deformation has been observed (*Pritchard and Simons, 2002*). Here we provide more details of our observations of Lascar, including higher quality interferograms made with DEMs from SRTM, and discuss the possible explanations for the lack of deformation.

Lascar was first observed to be active in 1848, and the activity intensified in 1984. Since then, there have been several cycles of activity culminating in eruptions that have been monitored on the ground, in the air, and in space (*Oppenheimer et al., 1993; Matthews et al., 1997; Wooster and Rothery, 1997; Wooster, 2001*). Lascar has persistent fumarolic activity and an unusual harmonic tremor (probably related to shallow hydrothermal circulation) was detected by a short-lived seismic array (*Hellweg, 1999*).

The biggest eruption in the central Andes during the last century occurred at Lascar between April 19-20, 1993, and was the largest at Lascar in over 9000 years (*Gardeweg et al., 1998*). That eruption produced 18.5 km² of pyroclastic flows, an ash cloud that rose 20 km into the atmosphere, and had a Volcano Explosivity Index (VEI) of 4, with between $1-4 \times 10^8$ m³ of material ejected (*Francis et al., 1993; Smithsonian Institution, 1993b; Gonzalez-Ferran, 1995; Deruelle et al., 1996; Sparks et al., 1997; Wooster and Rothery, 1997; Matthews et al., 1997; Denniss et al., 1998*). We do not see any deformation in two interferograms that span this large eruption (Figure 1.6). Given the sensitivity of our measurements (about 1-2 cm) and a source volume of 1×10^8 m³, the magma chamber would need to be more than 40 km deep (below local relief) for this amount of material to be removed and no deformation

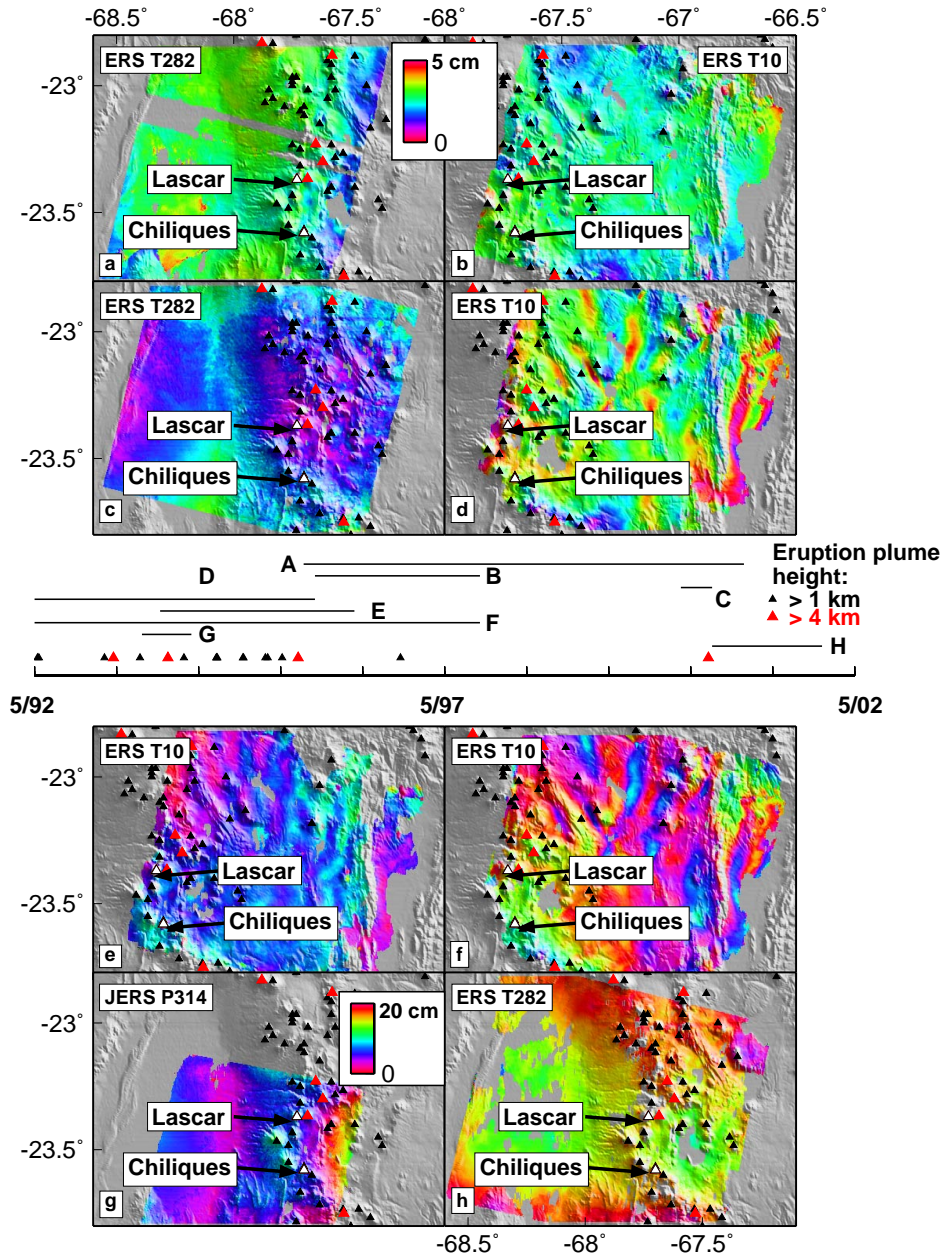


Figure 1.6: Interferograms showing no deformation at Lascar or Chiliques (both shown as white triangles) from two tracks of radar data from ERS and one path of data from JERS. In the center of the figure, the time period of the interferograms and eruptions of Lascar are shown (*Matthews et al., 1997; Smithsonian Institution, 1994a, 1995, 1997a, 1998a,b,c, 2000a*). There were no eruptions at Chiliques during the time interval, but a thermal anomaly was reported there in early 2002, see text. Interferograms from ERS orbital track 282 are shown in a, b, and h; from ERS orbital track 10 in b, d, e, and f; and JERS path 314 in g. Atmospheric artifacts are apparent in most images, and are similar in d and f which share an identical scene. Atmospheric artifacts are also apparent in the JERS data at the volcanic peaks to the southwest of Lascar, which we do not believe to be deforming. Deformation in the Salar de Atacama is visible in a, and shown in more detail in Figure 1.9. Other symbols are the same as in Figure 1.1.

observed (assuming a spherical source in an elastic half-space). There is uncertainty in the volume estimate (and therefore the minimum depth) for at least three reasons: (1) the amount of erupted products is uncertain by at least a factor of 4, (2) the conversion of the porous erupted volume to dense rock equivalent (DRE) is not precisely known, and (3) the relation between sub-surface volume change and surface deformation depends on the source geometry (*Delaney and McTigue, 1994*) as well as the rheological structure of the crust.

The trade-off between DRE volume and source depth for a spherical source is shown in Figure 1.7 assuming 1 or 5 cm accuracy of the deformation measurements. Realistically, the DRE volume might be as low as $4\text{-}5 \times 10^7 \text{ m}^3$, giving a minimum depth of 25-30 km for a 1 cm sensitivity to deformation. Even though there is large region of decorrelation around the edifice in these interferograms because of the erupted ash, the volume of material removed from the ground is so large that the region of decorrelation does not impact our estimate. We do not observe any deformation or change in the coherence as a function of time over the pyroclastic flows in post-eruption interferograms that might be caused by cooling/solidification of the flow (as observed in the thermal infrared satellite data, *Wooster, 2001*), although the InSAR observations have poor temporal resolution.

We do not observe any deformation at Lascar in the time interval between May 1992, and December 2001 (Figure 1.6). This time interval spans several small eruptions (VEI of 2 or less, *Simkin and Siebert, 1994*), with the largest occurring on July 20, 2000, July 20, 1995, and December 17, 1993, (e.g., *Smithsonian Institution, 1993c, 1994b, 2000b; Matthews et al., 1997; Wooster and Rothery, 1997; Wooster, 2001*). For these smaller eruptions, the correlation around the edifice is greater than for the April 1993 eruption, but even over the shortest time period we have studied with no known deformation (10 months), we are unable to take any measurement on the edifice. Even though the eruptions between 11/1993 and 12/2000 are small, we can rule out shallow spherical sources, but can place upper limits on how deep the source is. Assuming appropriate volumes for the largest eruptions during the observed time interval (VEI 2 - $10^6 - 10^7 \text{ m}^3$, *Simkin and Siebert, 1994*) a spherical

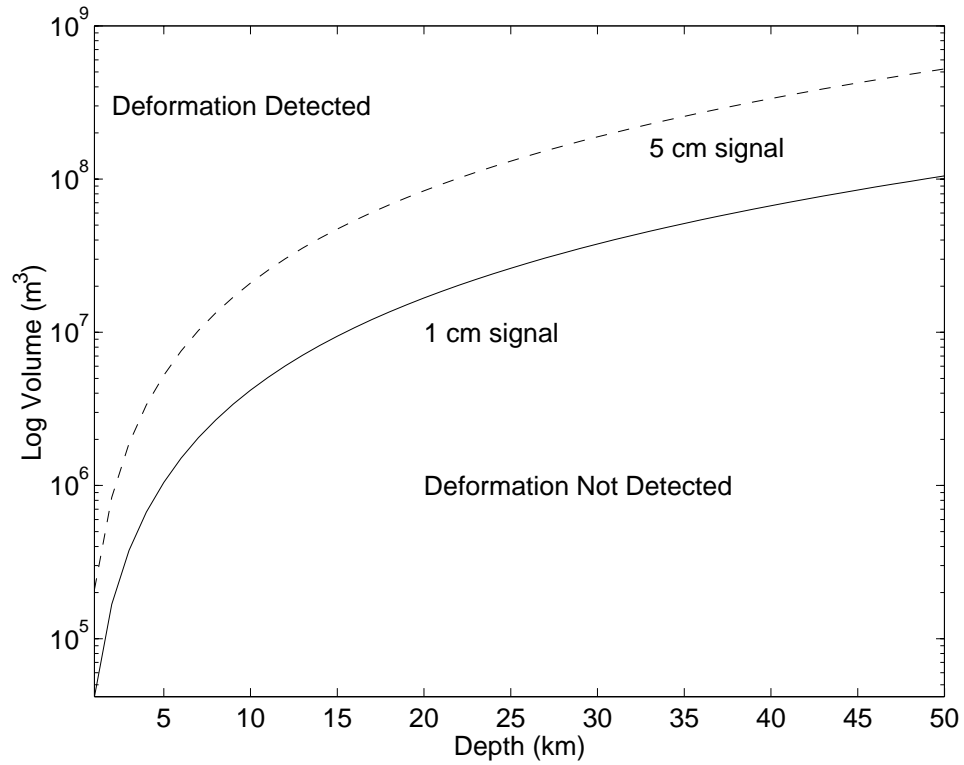


Figure 1.7: Required volume change at a given depth necessary to produce a maximum surface deformation of 1 and 5 cm. We estimate the accuracy of the ERS measurements to be 1 cm and the JERS measurements to be 5 cm (because of the larger atmospheric contamination of these scenes). We assume a constant amplitude signal for detection for sources at all depths, although, in reality, the detection of a deep source is easier than a shallow one because of the larger spatial scale of the deep source should make it easier to differentiate from atmospheric effects.

point source in an elastic half-space must be deeper than 5 and 12 km (respectively, for the two source strength extremes), given that we could observe surface deformation of 1 cm. We have tried to further constrain deformation associated with the December 17, 1993, eruption by forming interferograms with data from the JERS satellite (spanning 4/1994-8/1993 and 4/1994-7/1993, shown in Figure 1.6 and in the Appendix). We think the JERS data covering the eruption at Lascar is contaminated by atmospheric effects since we observe a signal at several peaks (residual topography) that are not deforming according to our ERS observations. The JERS data is useful because of the shorter timespan, but because the accuracy of the JERS measurements is of order 5 cm (because of the greater atmospheric contamination), the constraint on minimum depths of the magma chamber are superseded by the ERS observations (2-7 km, Figure 1.7).

It is hard to understand why there is no visible deformation at Lascar, because several lines of evidence suggest shallow activity at Lascar – the rate of outgassing, the size of the collapse craters (*Matthews et al.*, 1997) and the seismic data (*Hellweg*, 1999). Furthermore, there must be subsurface magma movement associated with the arrival and removal of material in the several eruptions. Of course, the magma that was erupted could have been emplaced (with accompanying ground deformation) prior to our observations during periods of activity in the 1980's and early 1990's. However, the removal of the material in the eruptions (particularly the 10^8 m³ removed in April, 1993) should have caused surface deformation. For example, subsidence was observed associated with the 1997 eruption of Okmok volcano, Alaska (*Mann et al.*, 2002; *Lu et al.*, 2000b), and the 1991-1993 Etna, Italy eruptions. At Etna, it is unclear whether the observed subsidence is equal to the volume extruded. The rate and volume of lava extruded are known (*Stevens et al.*, 1997) (about the same as the 4/1993 Lascar eruption – 2×10^8 m³), but there is controversy over the subsidence volume for two reasons: (1) the data could have significant atmospheric contamination, reducing the magnitude of the deformation by a third or more (*Delacourt et al.*, 1998; *Beauducel et al.*, 2000); and (2) the depth of the deformation source could be between 6-16 km (*Massonnet et al.*, 1995; *Bonaccorso*, 1996; *Lanari et al.*, 1998; *Delacourt et al.*, 1998).

Because of the trade-off between source depth and volume, this allows for a range of volumes. In spite of the controversy, all the estimates of the subsidence volume agree with the erupted volume to a factor of 5 or so. However, it should be noted that the Okmok and Etna lava eruptions might be fundamentally different from the explosive eruptions at Lascar.

We offer three possible explanations for the lack of observed deformation: 1) The first possibility has already been mentioned – the source is deep, at least 25 km (or 20 km below sea level) for the April 1993 eruption. Depending on the DRE of the eruption, a depth of more than 40 km might be required. Petrological constraints on the depth of the magma chamber for the Soncor eruption of Lascar (26 ka, 8 km³ of material erupted) (*Gardeweg et al.*, 1998) indicate a shallow depth (5-6 km, *Matthews et al.*, 1999), although earlier work favored a deeper depth (12-22 km, mean 16.6 km, *Matthews et al.*, 1994). Petrological depth constraints must be interpreted carefully because magma chambers might exist at multiple levels at a given edifice and the geochemical data might only be sensitive to the final (and shallowest) reservoir. For example, the April 1993 eruption is different from the eruptions in 1986 and 1990 in that its eruptive products are more silicic, indicating the involvement of a more evolved magma (*Matthews et al.*, 1997), and perhaps supporting the existence of multiple chambers or a single large and heterogeneous chamber. The fact that the large magnitude Soncor eruption did not initiate crater collapse, could indicate the existence of a large, strong, and possibly deep magma chamber (*Gardeweg et al.*, 1998). The magma chamber at Lascar appears to be in contact with a particular carbonate formation (*Matthews et al.*, 1996). If the local depth of that formation could be found, there would be an additional constraint on chamber depth. The only seismic constraints on chamber location are a swarm of volcano-tectonic events located at 4.5 km one week after the April 1993 eruption (*Matthews et al.*, 1997). It is unclear whether a deep magma chamber (> 20 km deep) would be consistent with the shallow lava dome model for the cyclic eruptive pattern at Lascar (see below).

2) The chamber (or conduit – whatever was holding the magma) behaved rigidly and did not deform when the erupted volumes were removed. While we do not

favor this possibility, we note that gravity measurements at several volcanoes (that are more mafic, with less viscous magmas) appear to indicate magma movements without surface deformation, possibly as the magma evacuates pore space or moves through a rigid conduit (*Rymer et al.*, 1993; *Watanabe et al.*, 1998; *Fernández et al.*, 2001). This mechanism will probably not work at Lascar, where the viscous magmas are likely coupled to the surrounding rock, and any magma movement should cause deformation.

3) The absence of observed deformation at Lascar can be understood using a model for the Lascar eruption cycle developed by *Matthews et al.* (1997). The April 1993 and other eruptions at Lascar (particularly those on 9/16/1986, 2/20/1990, and 12/17/1993) are believed to be triggered by movements of the surficial lava dome. In the model of *Matthews et al.* (1997), a lava dome is formed and degasses energetically, but eventually subsides as the magma loses volume. The subsidence as well as loss of magma vesicularity and hydrothermal mineralization reduces the rate of degassing and causes the pressure in the magma chamber to build, eventually leading to eruption. The lava dome has been observed to subside in photographs, and the thermal emission of the fumorales monitored by satellite has been observed to drop before the eruptions in 1986, 1990 and 1993, as expected if the degassing rate decreases (*Wooster and Rothery*, 1997).

Because of the poor temporal resolution of InSAR, one possible explanation for the observed lack of deformation at Lascar is that the lava dome collapse and pressure build up canceled the pressure release during the eruption, such that there is no net deformation. For example, our interferograms spanning the April 1993 eruption begin on May 2, 1992, while satellite observations indicate that dome collapse and pressure build-up began in May-June 1992 (*Wooster and Rothery*, 1997). Similarly, our interferograms spanning the December 1993 eruption begin on November 13, 1993, while satellite observations indicate that pressure build up likely began on December 12, 1993. Alternatively, a pressure build-up immediately following the eruption (and concomitant surface inflation) could have nearly canceled the co-eruptive pressure decrease and deflation. For example, rapid repressurization (hours-weeks) has been

observed in several shallow magma chambers (*Dvorak and Dzurisin, 1997; Voight et al., 1999*). Following this eruption, the cyclic pattern appears to have been broken as no lava dome re-appeared and the correlation between radiant flux and eruptions is less coherent (*Wooster and Rothery, 1997; Matthews et al., 1997; Smithsonian Institution, 2000b; Wooster, 2001*). The departure from the cyclic pattern may be a result of the large April 1993 eruption changing the plumbing of the volcano. Nonetheless, the July 20, 2000, event might have followed the previous pattern and have been preceded by a radiance decrease (associated with a shut-off of degassing and increase in magma pressure) on June 23, 2000. Once again, the InSAR measurements begin much earlier, so they cannot resolve the temporal evolution. This ambiguity in interpretations is directly attributable to the lack of good temporal coverage of the SAR imagery.

1.4.3.2 Irruputuncu

Two eruption plumes were recorded on September 1 and November 26 1995 (VEI 2) (*Smithsonian Institution, 1997b*) at this stratovolcano in Chile. *Zebker et al. (2000)* made a 70-day interferogram that spanned the September 1 event, but saw no deformation. We made several interferograms spanning 5/1992-5/1996, and did not observe any deformation at Irruputuncu (Appendix). Assuming the sensitivity to deformation is 1 cm, the magma chamber would need to be more than 7-15 km deep (Figure 1.7) for eruptions of this size to be undetected.

1.4.3.3 Aracar

An ash plume was observed at this stratovolcano in Argentina on March 28, 1993 (VEI 2) (*Smithsonian Institution, 1993a*). No clear deformation signal is observed in several interferograms spanning 5/1992-12/2000, although there is clear atmospheric contamination in the single interferogram spanning the eruption (5/1992-10/1997, see the Appendix). Assuming the sensitivity to deformation is 3 cm (because of the larger atmospheric contamination) for this interferogram, the magma chamber would need to be more than 4-10 km deep (Figure 1.7) to explain the lack of deformation.

1.4.3.4 Sabancaya

It is possible that the inflation we see near Hualca Hualca is related to activity at Sabancaya, and local seismic data might provide evidence of a relationship. The eruptions of Sabancaya have been associated with seismic activity and the largest earthquake was a $M_s \sim 5$ event on July 23, 1991 (*Smithsonian Institution*, 1991b). A seismic array installed in June 1990, found a concentration of earthquakes on the northeast side of Hualca Hualca, about 10 km from Sabancaya, 4-7 km below sea level, and that the earthquakes migrated to the south in August and September 1990 (*Lazo et al.*, 1991). It is possible that the seismic activity in this location is related to the inflation that we observe during later time periods, as they are both in roughly the same location.

Any deformation associated with the eruptions of Sabancaya would be convolved with the deformation NE of Hualca Hualca. Figure 1.5 shows some of the interferograms at Sabancaya/Hualca Hualca spanning the series of eruptions that followed the renewal of activity at Sabancaya in 1990-1992. There is no unambiguous evidence for deflation of the magma chamber at Hualca Hualca or beneath Sabancaya. There is possibly less than a fringe of subsidence in the interferograms in Figure 1.5c and 1.5e, but the effect could be atmospheric. Furthermore, detailed study of these interferograms will not be possible until the effects of the M_w 8.4 Arequipa earthquake can be properly removed.

There is an east-west elongated pattern of subsidence in the interferogram spanning 11/1995-12/2001 (Figure 1.5e, see Figure 1.8b for a more detailed view), although the deformation is constrained to have occurred between 10/2/1997-1/10/1999 or 7/9/2001-12/21/2001. This subsidence does not appear related to the magma chamber deformation imaged in the other interferograms, and might be related to hydrologic activity (discussed below). The largest eruption during the time period for which data is available was in May, 1995 and had a VEI of 3 (between 10^7 and 10^8 m³). If the magma chamber was more than 15 km below the surface, the deformation signal might be below the 1 cm threshold (Figure 1.7). Our modeling suggests that the

chamber is 15-20 km deep below Hualca Hualca (see Chapter 2), so if the magma came from there, and the erupted volume is near the low end of the possible range, subsidence might not be observed. The rate of inflation does not seem to be directly affected by the eruption, although the temporal resolution is poor (see Chapter 2). While not temporally well constrained, inflation of Hualca Hualca seems to have stopped in 1997 (Figure 1.5 and Chapter 2), perhaps related to the large eruption in May, 1997. Sabancaya has continued to emit gas, but no large eruptions have been reported since the cessation of inflation at Hualca Hualca.

1.4.4 Non-volcanic deformation

1.4.4.1 Salars

The arid central Andes has numerous large salars (salt flats, e.g., *Díaz*, 1988), and we observe apparent heterogeneous deformation (mostly uplift, if deformation is vertical) at several of them (Figures 1.9 and 1.10). Nearly every major salar between 22°-27°S either appears to deform or to be decorrelated. Salar deformation was neither expected nor the focus of our survey. As a result, we only have a few interferograms showing deformation at several salars, and so our results should be thought of as preliminary and motivation for further study.

For three salars (Salar de Arizaro, Salar de Rio Grande, and Salar de Llullaillaco), we observe a signal with a consistent sign in three interferograms (spanning 7/1995-10/1997, 8/2000-10/1996, 12/2000-5/1996), although the spatial character in each is slightly different (perhaps because of atmospheric contamination?). We do not think the entire signal is atmospheric because the deformation ends abruptly at the edge of the salt at the Salar de Atacama and the Salar de Arizaro (Figure 1.9). This feature is not an unwrapping error, as it appears in interferograms made with no unwrapping using the 2-pass method. We do not think that the signal is a permanent atmospheric effect above the salar because there is no signal whatsoever correlated with the salars in a short time period interferogram (8/1995-5/1996). While it is possible that the deformation seen at the three salars (Salar de Arizaro, Salar de Rio Grande,

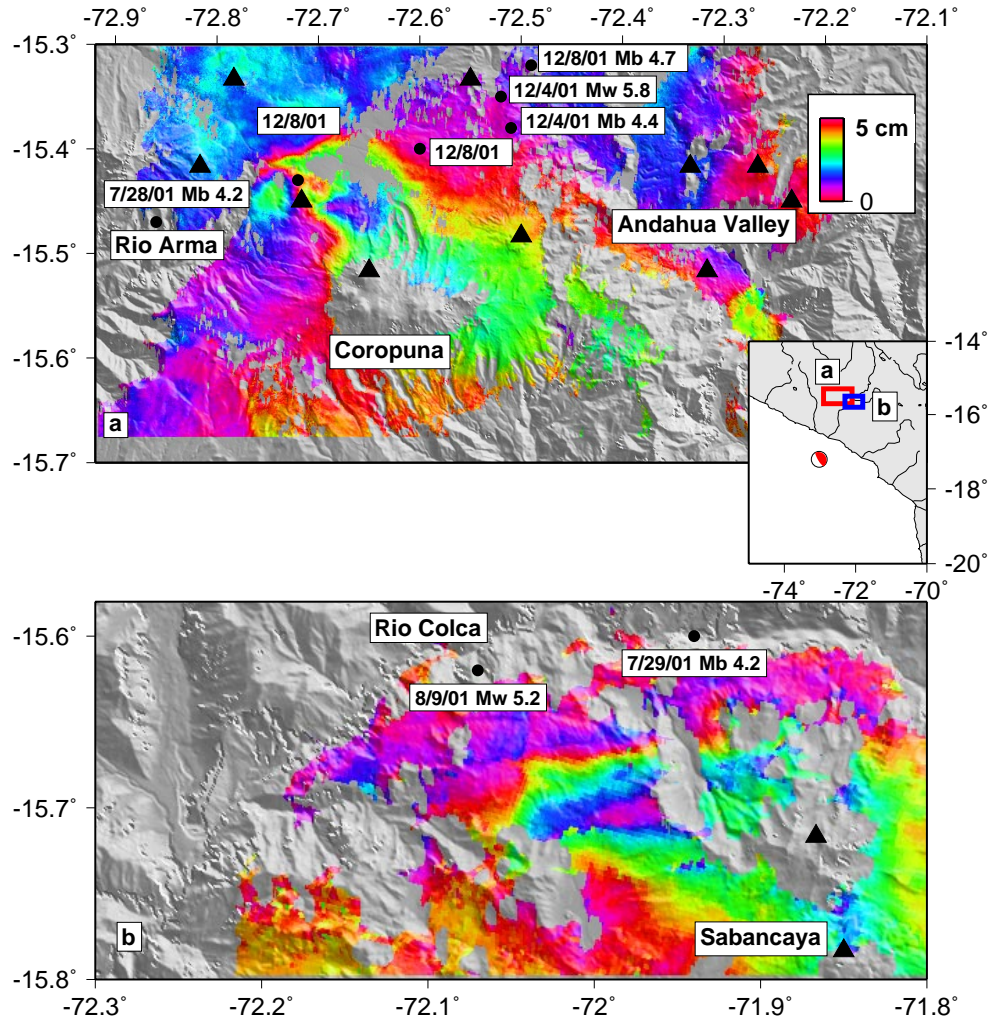


Figure 1.8: Inferred hydrological deformation near volcanic areas possibly related to the Arequipa earthquake (location shown in the inset map). a. Interferogram spanning 4/9/1996-1/9/2002 showing deformation near Coropuna volcano and the Arma river. The northern part of the pattern shows subsidence in the river valley, but the maximum subsidence is on the east side of an unnamed lava dome (shown as the black triangle in the middle of the deformation pattern). A small amount of uplift is observed on the west side of the lava dome. Shallow earthquakes (< 50 km depth) from the appropriate time period are shown as black circles with dates and magnitudes shown, when available. All locations are from the NEIC catalog, and have depths set at 33 km. b. Interferogram spanning 11/2/1995-12/21/2001 showing the more geometrically simple deformation pattern near Hualca Hualca and the Colca river. Shallow earthquakes are shown as in a.

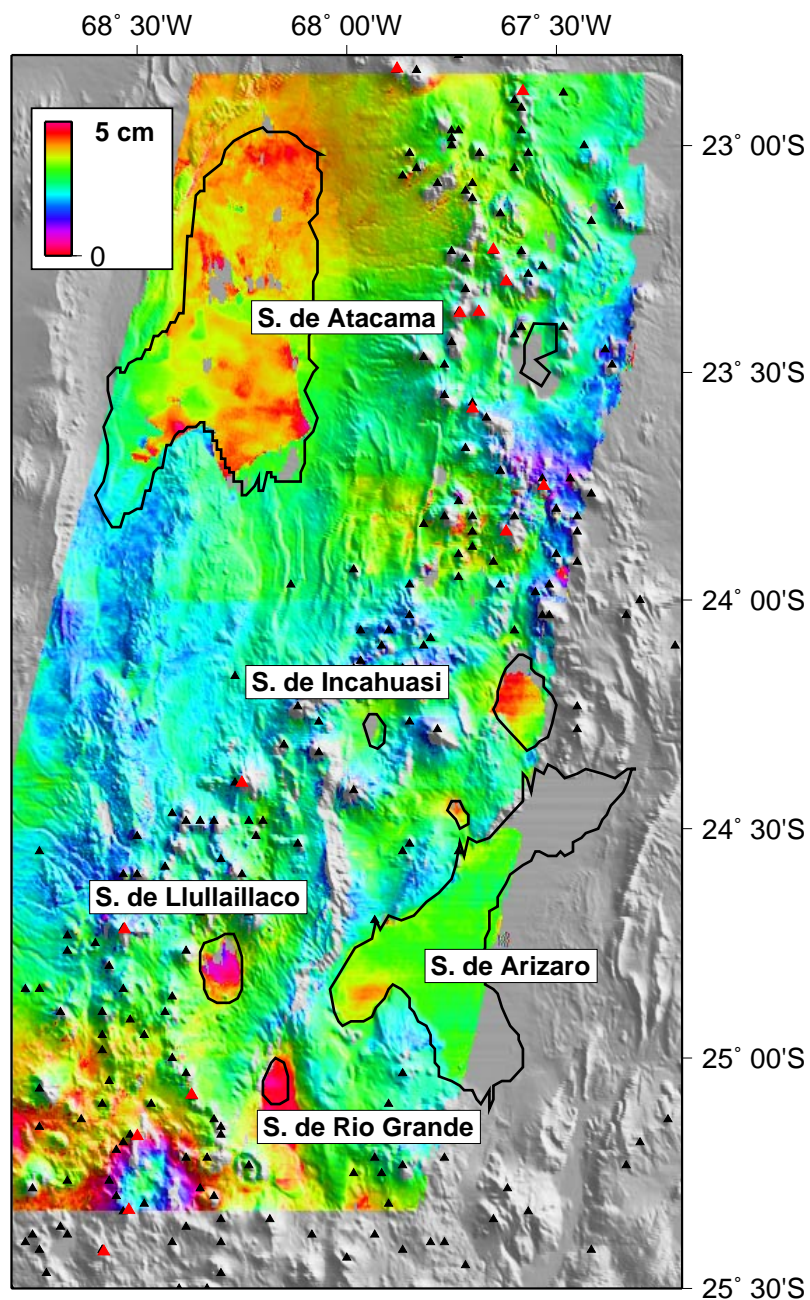


Figure 1.9: Interferogram spanning 12/24/2000-5/18/1996 showing heterogeneous deformation at several salars. Deformation ends abruptly at the edge of the salt flat at the Salar de Arizaro and the Salar de Atacama. We assume that deformation is vertical, and so there is mostly inflation at the salars, although there is some localized subsidence on the Salar de Atacama possibly related to water extraction (S. Kampf, personal communication, 2001). The red at the lower left edge of the interferogram is from Lazufre. Figure 1.10 shows a portion of the same interferogram further south.

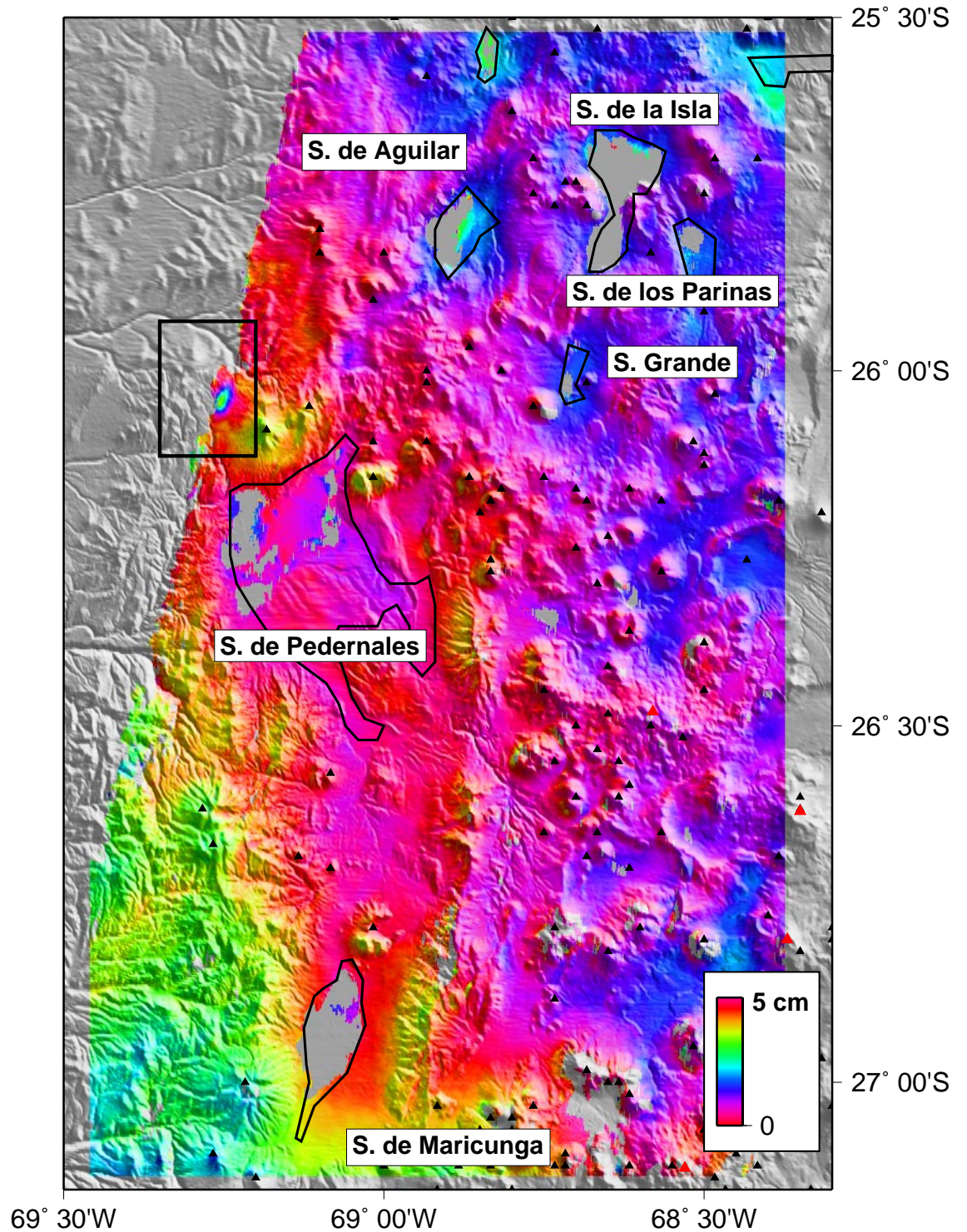


Figure 1.10: Interferogram spanning 12/24/2000-5/18/1996 showing limited deformation at several salars, as well as a possible shallow earthquake near the western edge of the interferogram at 26° (the boxed region is shown in Figure 1.11). These salars show more decorrelation than the ones further north, perhaps related to the presence of water on the surface. There appears to be inflation next to some of the areas of decorrelation.

and Salar de Llullaillaco) occurred during a single episode during the common time period (10/1997-5/1996), evidence from the Salar de Atacama indicates at least one other independent time period of deformation. At the Salar de Atacama, deformation is seen in interferograms spanning 12/2001-8/2000 and 12/2000-5/1996 but not in interferograms spanning 8/1995-5/1996 and 8/2000-3/2000, so the simplest interpretation is that deformation occurred between 12/2000-8/2000. Obviously, more frequent observations are needed to constrain the temporal evolution of the deformation.

There are at least three possible causes of the deformation that we observe: 1) Rainfall or subsurface water flow into the basins caused expansion of hydroscopic clays and salts, as inferred to have occurred in the Salton Trough, California (*Gabriel et al.*, 1989). The fact that the observed inflation ends abruptly at the edge of the salt surface would be consistent with this observation. 2) Inflation may be due to subsurface groundwater recharge into a permeable layer that acts to lift the salar surface coherently. A material contrast between the salt and the surrounding material would cause the deformation to end abruptly at the edge of the salt at the Salar de Atacama and the Salar de Arizaro. We suppose that the hydraulic head does not allow the water to collect in only one area, and so that it must quickly spread across the entire salar, causing the broadly distributed deformation pattern that we observe. 3) The salar surface moves up and down due to subsurface water motion caused by tides. Water levels in wells in the Salar de Atacama are seen to fluctuate in response to the tides (C. Ramirez, personal communication, 2002), and this tidal response is expected at any confined aquifer (e.g., *Bredehoeft*, 1967).

Because the surface maintains interferometric coherence at many of the salars, we do not think that surface processes are causing the signal, although several salars show decorrelation, possibly the result of standing water on the salar surface. Even at many of the salars with decorrelation, there is apparent inflation of the surface that is maximal near the decorrelation and diminishes with distance, possibly related to diffusion away from the surface water source. Spatial complexities in the pattern of deformation might be atmospheric effects, or real difference in ground deformation

caused by variations in the thicknesses of the deposits or subsurface faults. Subsurface faults without surface topographic expression have been imaged in the Salar de Atacama, and likely influence groundwater flow (*Jordan et al.*, 2002).

There is a north-south difference in the salar decorrelation, with the salars north of 25°S showing little decorrelation (Figure 1.9) while those south are almost all decorrelated (Figure 1.10) during the same time period. We do not know the cause of this north/south difference, but note that there is more snowfall during the winter in the south (*Vuille and Ammann*, 1997), although there does not appear to be major change in summer precipitation between these regions.

1.4.4.2 A shallow earthquake?

In addition to showing possible salar deformation, Figure 1.10 shows an elliptically shaped deformation pattern (about -4 cm LOS, mostly due to uplift) at about 26.04°S and 69.25°W. This pattern has been observed in independent interferograms from two different tracks (both shown in Figure 1.11), and by forming overlapping interferograms of the area between 10/1993-8/1999, we constrain the deformation to have occurred either between 3/14/1997-10/10/1997 or 5/28/1999-8/6/1999. We are not aware of any hydrothermal activity or anthropogenic sources of deformation (wells, mines, etc.) in the vicinity of the deformation pattern. Therefore, we think it possible that the fringe could correspond to an earthquake. Figure 1.11 shows the epicenters for the closest earthquakes in the ISC and NEIC catalogs to the deformation pattern during the time period when deformation could have occurred. The epicenters of the earthquakes on 7/27/1997 and 7/25/1995 are closest to the deformation (with M_b 4.3-5), but according to the seismic data, both earthquakes have depths exceeding 20 km, with many solutions favoring depths between 40-50 km. We invert the deformation for the best fitting point source using the Neighbourhood Algorithm algorithm in an elastic half-space (e.g., *Sambridge*, 2001; *Lohman et al.*, 2002). Because there are trade-offs between several parameters (for example, rake and dip, *Cervelli et al.*, 2001; *Lohman et al.*, 2002), a range of thrust mechanisms can explain the data, but the best fitting parameters are: depth 3-4 km, dip 62, strike 191, rake 100, and

M_w 5.1. The fit to the data is not significantly improved if a finite fault with several subpatches (with the dip, strike and rake fixed to the values from the point-source solution) is used instead of the point source. We have not attempted to model the seismic data from 7/27/1997 and 7/25/1995 because of the low signal-to-noise ratio of the data (the closest stations were about 500 km away as part of a temporary array, *Chmielowski et al.*, 1999). On November 10, 1996 the NEIC and ISC catalogs indicate that there was a $M_b \sim 4.5$ crustal earthquake (depth solutions between 28-58 km) in about the same location (25.84°S 69.05°W), but interferograms show no obvious deformation, indicating that if the location is approximately correct, this earthquake was not shallow.

Earthquakes in this region are very poorly located, and so it is possible that some event in the catalog actually does match this earthquake, but the depth is off by more than 20 km, or that this earthquake was totally missed. Although there are many tectonic features in the continental area between the western cordillera of the Andes and the coast, shallow earthquakes in this region were not seen in early local studies (e.g., *Comte et al.*, 1994; *Delouis et al.*, 1996) and have only been detected recently by a temporary array (PISCO'94) that operated for about 100 days (*Graeber and Asch*, 1999). If the source of deformation is a shallow earthquake, it might indicate that there are many more shallow earthquakes recorded annually, but that the depths are miscalculated in the global catalogs.

1.4.4.3 Post-seismic hydrological activity?

Following the June 23, 2001, M_w 8.4 Arequipa earthquake, there were reports of increased fumarolic activity at El Misti volcano, (about 30 km from Hualca Hualca, Geological Society of America News Release No. 01-66, December 12, 2001, <http://www.geosociety.org/pubntrst/pr/01-66.htm>). We do not observe any deformation at El Misti, but we do observe deformation (a few cm in the LOS, primarily subsidence) to the NW of Coropuna volcano near the Arma river and NW of Hualca Hualca near the Colca river (Figure 1.8). We think that the source of deformation is shallow – for example, at Hualca Hualca the pattern is spatially smaller, and in a

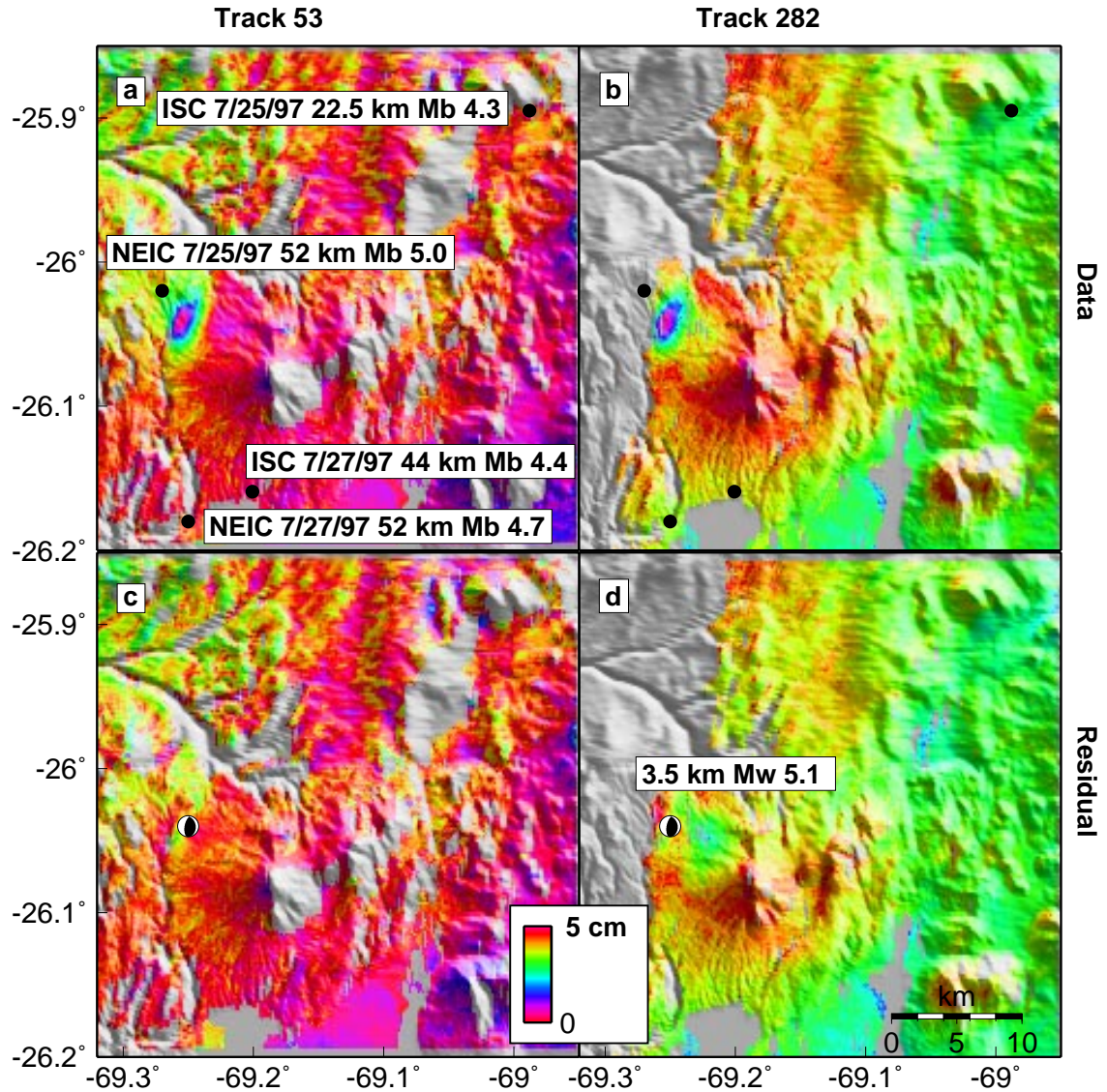


Figure 1.11: Interferograms and residuals from two orbital tracks showing a possible shallow earthquake. a. Interferogram from track 53 spanning 3/14/1997-8/6/1999. b. Interferogram from track 282 spanning 8/12/1995-12/24/2000. The circles show the locations, depths, and body-wave magnitudes (M_b) of the earthquakes closest to the deformation in the NEIC and ISC catalogs within the timespan when deformation occurred (3/14/1997-10/10/1997 or 5/28/1999-8/6/1999). c. Residual from track 53 from our best fitting point-source model with the mechanism shown at a depth of 3.5 km and M_w 5.1. d. Residual from track 282. The RMS misfit for both interferograms is about 0.5 cm.

different location than the deformation we infer to be from the deep magma chamber. At Hualca Hualca, the deformation is constrained to have occurred between 10/2/1997-1/10/1999 or 7/9/2001-12/21/2001, because it is not observed in interferograms spanning the other time periods. Therefore, the deformation at Hualca Hualca did not occur at the same time as the earthquake (6/23/2001) or its largest aftershock (M_w 7.6 on 7/7/2001), but might have been a post-seismic response during the first 6 months after the earthquake. At Coropuna, the deformation must have occurred between 10/21/1997-1/9/2002.

Although the exact timing is poorly resolved, we think that the deformation may be related to the Arequipa earthquake or its aftershocks, because this deformation seems unique to this time interval (we have interferograms of both areas starting in mid-1992). We hypothesize that the deformation may result from consolidation of a porous (most likely volcanic) deposit and expulsion of fluid, mostly to the nearby rivers, although there is limited uplift in the Coropuna interferogram. It is possible that some of the deformation is due to shallow earthquakes (Figure 1.8), but these are so poorly located in this region that this is difficult to test. The hypothesis of post-seismic pore pressure increase has been proposed to explain the increased streamflow at Sespe Creek, CA, following several earthquakes (*Manga et al.*, 2003). Considering that the sources of deformation are about 200 km from this M_w 8.4 earthquake, this mechanism is plausible considering previously established distance-magnitude relations for the proposed phenomena (*Manga*, 2001). We are trying to test our hypothesis by seeing if there is a change in streamflow immediately following the earthquake in the Arma-Chichas-Ocoña and/or Colca-Majes-Camaná river systems. A further requirement to test this hypothesis is to map the location of porous deposits in these areas.

1.4.4.4 Sources of speculation

In addition to the clear sources of deformation we describe above, our survey reveals several other more speculative deformation sources that might merit further attention.

Figure 1.12a shows two shallow sources of deformation in southern Peru of un-

known origin. Four interferograms spanning May 1992 to April 1996 show localized uplift in the Andahua Valley near Laguna de Chachas (Figure 1.12a and Appendix). The deformation pattern could be seasonal: about 3 cm of deformation in the LOS is observed between May 1995 and May 1992, and additional 1.5 cm between May 1995 and April 1996, and no deformation is seen between September 1995 and October 1997. About 1 cm of subsidence is observed in interferograms spanning April 1996 to January 2002. There is also the possibility of a longer wavelength uplift signal in the valley, but we suspect that this might also be due to atmospheric contamination. Although this valley contains numerous scoria cones (*de Silva and Francis, 1991*), based on the location and shape of the localized deformation, we think that it is most likely caused by shallow subsurface water movement, perhaps related to Laguna de Chachas.

Figure 1.12a also shows a very localized region of subsidence between the Andahua Valley and Coropuna volcano, on the slopes of Cerro Allipampa near Quebrada Quiñual. The deformation is only detected clearly in a single interferogram, but other interferograms of the area spanning the same time interval are much more noisy, so the small signal might not be visible. There are no known sources of deformation in this area (*i.e.*, mines, geothermal fields or earthquakes). The closest earthquakes are shown in Figure 1.12a and are located on the interplate interface at about 120 km depth. If the deformation is an earthquake, modeling it as a point source gives a depth of about 1 km, M_w 4.3 and the mechanism shown in Figure 1.12a. It is likely that an earthquake this small might not be included in the global catalogs, but because of the difficulty in viewing this deformation signal with InSAR, its exact origin remains a mystery.

Interferograms in the Appendix over the caldera Pastos Grande (*de Silva and Francis, 1991*) from track 282 reveal a sharp phase gradient near the caldera rim scarp. However, interferograms of the same region from track 53 over nearly the same time period do not contain the same features. Interferograms from track 282 also reveal possible subsidence at Cerro Quebrada Honda (dome) just south of the caldera Pastos Grandes (67.7°W, 22.0°S), but are also not observed in data from track 53.

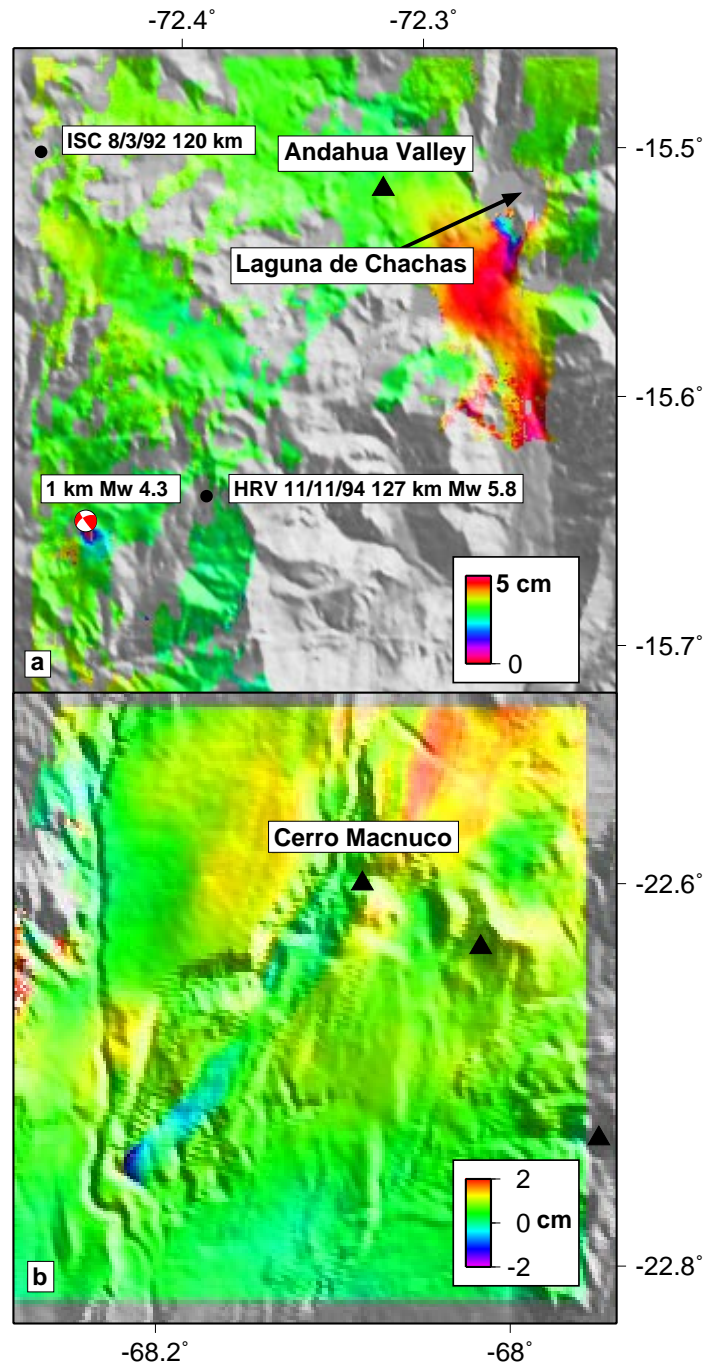


Figure 1.12: a. Deformation in an interferogram spanning 5/17/1992-5/30/1995 from southern Peru (track 225, frame 3933) of unknown origin. The uplift in the Andahua Valley is near a lake and might be hydrological, which the localized subsidence in the southwestern corner is located on a hill slope. We fit a point-source double couple to the localized subsidence in the southwestern corner, and the mechanism, magnitude and depth are shown. The circles show the locations, depths, and magnitudes (where available) of the earthquakes in this region during the period of observation, all of which are very deep and located on the plate interface. b. Interferogram spanning 12/24/2000-5/18/1996 showing a long, narrow region of subsidence of unknown origin. It might be of hydrological origin related to nearby streams, ground slumping, or a lava flow from the nearby Cerro Macnuco, although no eruptions are known to have occurred in this area in recent times.

Furthermore, the track 282 interferograms indicate more moderate subsidence at the Sol de Mañana geothermal field (*de Silva and Francis, 1991; Gonzalez-Ferran, 1995*), but could also be local atmospheric effects do to geothermal steam as suggested for the Cerro Prieto geothermal plant, Mexico (*Hanssen, 2001*). All of these effects could be due to atmospheric contamination in data from our acquisitions of track 282. Two independent interferograms from track 282 reveal a spatially elongate region of heterogeneous subsidence that might be related to shallow hydrogeological processes or a subsiding lava flow near Cerro Macnucu (68.1°W , 22.6°S), a caldera listed by *de Silva and Francis (1991)* with a question mark (Figure 1.12b). All of the sources mentioned in this paragraph lie within the Altiplano-Puna Magmatic Complex, and possible long-wavelength, low amplitude deformation associated with intrusion or melting of this large magmatic body are being studied by *Fialko (2002)*.

1.5 Conclusions

Over the 5-10 years for which data is available, we can detect deformation at only 4 of the almost 900 edifices surveyed, although more subtle deformation might also be occurring below our detection threshold. Such results would involve months to years to accomplish if we were confined to ground measurements. Furthermore, ground surveys might not have detected the volcanic sources because they were not listed as “potentially active” volcanoes or the non-volcanic deformation since such deformation was not predicted.

Clearly, at silicic stratovolcanoes, like those in the central Andes, there are different definitions of “active”: those with eruptions in the last 10,000 years (44 volcanoes, *de Silva and Francis, 1991*), fumarolically active (15 volcanoes), centers with a measurable thermal anomaly (2 volcanoes), actively deforming (4 volcanoes), and actively erupting (4 volcanoes in the 1990’s). Another criteria – seismically active – can not be applied in the central Andes because of the lack of data. This and other InSAR surveys (*Lu et al., 2002c; Wicks et al., 2002; Lu et al., 2000c; Amelung et al., 2000*) indicate that the different definitions of activity do not completely overlap. Moreover,

the manifestations of activity (fumaroles, thermal anomalies, and deformation) are temporally variable, so that all “potentially active” volcanoes need to be monitored regularly for temporary bursts of activity. For example, only two of the four centers of deformation were active during the entire time period, and even the deformation at these centers (Uturuncu and Cerro Blanco) appears time-dependent. We also found that the thermal anomaly at Chiliques was transient (less than 18 months). The eventual goal is to determine which “active” volcanoes pose a threat.

The low number of deforming volcanoes in the central Andes relative to the total number surveyed should not be considered representative of all volcanic arcs in the world. For example, the also remote Alaskan/Aleutian arc has about the same number of volcanoes in the Smithsonian database as the central Andes (about 80), but many more historic eruptions (41 compared to 17, *Miller et al.*, 1998; *Simkin and Siebert*, 1994; *Smithsonian Institution*, 2003), and more actively deforming (9 compared to 4, *Lu et al.*, 1997, 2000c,b,d, 2002c,b,a; *Price*, 2002; *Mann and Freymueller*, 2003). The lower level of activity in the central Andes might be related to the fact that the crust is much thicker there (50-70 km) than in Alaska, or the composition of the lavas (there are more large mafic volcanoes in Alaska) (*Miller et al.*, 1998; *Simkin and Siebert*, 1994; *Smithsonian Institution*, 2003). The level of activity in the central Andes is more comparable with the other active Andean chains, the northern Andes (6°N-2°S) and the southern Andes (33-50°S). The number of historic eruptions in the central Andes (17) is similar to the number in the northern Andes (15), although slightly less than the southern Andes (29) (*Simkin and Siebert*, 1994; *Smithsonian Institution*, 2003). The number of eruptions between 1990-2000 is about the same in the central (4), northern (5) and southern (6) Andes, and lower than the number in Alaska/Aleutians (17) (*Smithsonian Institution*, 2003).

The lack of deformation at Lascar (particularly the lack of subsidence associated with the eruptions) is mysterious, but has the potential to provide insight into the plumbing of this volcano. We can rule out injection or withdrawal of magma from a shallow magma chamber, unless the magma chamber can gain/lose magma without deforming – a process that is difficult to imagine for the silicic magmas at Lascar.

A deep magma chamber would explain the lack of deformation, but it must be at least 25 km (possibly much deeper) to explain the lack of deformation from the April 1993 eruption. Such a deep magma chamber might not be consistent with the fact that shallow movements of the lava dome seem to trigger eruptions in at least 1986-1993 (*Matthews et al.*, 1997). Considering the long periods between observations, inflation and deflation could nearly exactly cancel each other, especially if the eruptive process is cyclic or the magma chamber quickly re-pressurizes. In order to resolve this problem, further petrological and seismic studies of the magma chamber location should be undertaken, and InSAR measurements with greater temporal resolution must be acquired.

We did not observe subsidence associated with eruptions at Irruputuncu, Aracar, or Sabancaya, but these eruptions were smaller than those at Lascar, and so could plausibly be hidden by magma chambers only 10 km or so deep. In the case of Sabancaya, subsidence could have been masked by inflation from the magma chamber near Hualca Hualca, and in fact the eruptions might have been directly fed by this chamber. Other recent studies indicate many eruptions (smaller than the April, 1993 Lascar eruption) with no observed subsidence: Shishaldin, Alaska, 1999, VEI 3 (*Lu et al.*, 2000a); Makushin, Alaska, VEI 1 (*Lu et al.*, 2002b); Fogo, Cape Verde Islands VEI 2, but erupted 10^7 m³ of lava (*Amelung and Day*, 2002); Piton de la Fournaise, Reunion, VEI 1, but erupted 10^7 m³ of lava (*Sigmundsson et al.*, 1999). In the case of Fogo and Piton de la Fournaise, the lack of deformation was used to constrain the minimum magma chamber depth, and was supported by ancillary geophysical or geochemical data. In fact, the ocean islands Cape Verde, Reunion, and others (La Palma and El Hierro, Canary Islands) do not appear to have shallow magma chambers, perhaps related to landslides that disturb the thermal and mechanical structure of the islands (*Amelung and Day*, 2002).

Our results should encourage further monitoring of activity and assessment of possible hazard at the four actively deforming volcanoes. In this regard, the volcanoes of southern Peru have been the most closely studied because the population density is higher there than in other locations. The potential hazard from an eruption or

mudflows from Hualca Hualca, Sabancaya, or Ampato is serious (35,000 people live within the area of influence) and hazard assessment was undertaken by *Thouret et al.* (1995). Ashfall has already led to the deaths of livestock (*Smithsonian Institution*, 1988), and several people in the village of Maca have died from structural collapse caused by the July 1991, earthquake (*Smithsonian Institution*, 1991b). A seismic array that operated in the early 1990's has fallen into disrepair (M. Bulmer, personal communication, 2001), although many have recognized the need for permanent monitoring of activity at Sabancaya (*Gonzalez-Ferran*, 1995).